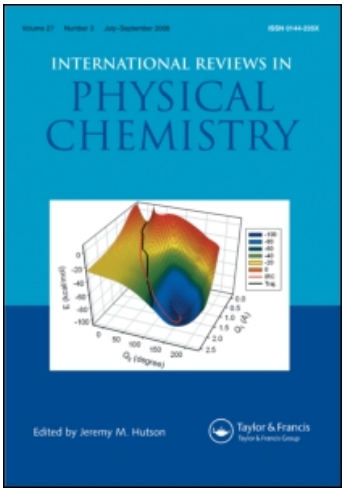

International Reviews in Physical Chemistry
Publication details, including instructions for authors and subscription information:
http://www.informaworld.com/smpp/title~content=t713724383

Ar ··· I 2 : A model system for complex dynamics

Alexei Buchachenko[a]; Nadine Halberstadt[b]; Bruno Lepetit[c]; Octavio Roncero[d]
[a] Laboratory of Molecular Structure and Quantum Mechanics, Department of Chemistry, Moscow State University, Moscow, Russia [b] LPQT-IRSAMC, Université Paul Sabatier and CNRS, Toulouse, France [c] LCAR-IRSAMC, Université Paul Sabatier and CNRS, Toulouse, France [d] Instituto de Matemáticas y Física Fundamental, CSIC, Madrid, Spain

Online publication date: 26 November 2010

To cite this Article Buchachenko, Alexei , Halberstadt, Nadine , Lepetit, Bruno and Roncero, Octavio(2003) 'Ar ··· I 2 : A model system for complex dynamics', International Reviews in Physical Chemistry, 22: 1, 153 — 202
To link to this Article: DOI: 10.1080/0144235031000075726
URL: http://dx.doi.org/10.1080/0144235031000075726

INT. REVIEWS IN PHYSICAL CHEMISTRY, 2003
VOL. 22, NO. 1, 153–202

Taylor & Francis
Taylor & Francis Group

$Ar \cdots I_2$: A model system for complex dynamics

ALEXEI BUCHACHENKO
Laboratory of Molecular Structure and Quantum Mechanics, Department of Chemistry, Moscow State University, 119992 Moscow, Russia

NADINE HALBERSTADT†
LPQT-IRSAMC, Université Paul Sabatier and CNRS, 118 route de Narbonne, 31062 Toulouse, France

BRUNO LEPETIT
LCAR-IRSAMC, Université Paul Sabatier and CNRS, 118 route de Narbonne, 31062 Toulouse, France

and OCTAVIO RONCERO
Instituto de Matemáticas y Física Fundamental, CSIC, Serrano 123, 28006 Madrid, Spain

We review spectroscopic and photodissociation dynamical studies in the region of the $B \leftarrow X$ transition of the $Ar \cdots I_2$ van der Waals complex, both below and above the dissociation limit of the $B(^3\Pi 0_u^+)$ state. This very simple system constitutes a prototype for a wide range of molecular processes: vibrational predissociation involving intramolecular vibrational relaxation, electronic predissociation, cage effect, ... Each of these processes has been or still is the subject of differing interpretations: intramolecular vibrational relaxation involved in the vibrational predissociation of this system can be in the sparse or statistical regime, vibrational and electronic predissociation are in competition and a direct, ballistic interpretation of the cage effect as well as a non-adiabatic one have been proposed. The study of the dependence of these dynamical processes on the relative orientation of the two partners of the complex (stereodynamics) is made possible by the coexistence of two stable $Ar \cdots I_2(X)$ isomers. Experimental as well as theoretical results are reviewed. Experiments range from frequency-resolved to time-dependent studies, including the determination of final state distributions. Theoretical studies involve potential energy surface calculations for several electronic states of the complex and their couplings and adiabatic as well as non-adiabatic dynamical simulations.

Contents

† E-mail: nhalbers@irsamc.ups-tlse.fr

International Reviews in Physical Chemistry ISSN 0144–235X print/ISSN 1366–591X online © 2003 Taylor & Francis Ltd
http://www.tandf.co.uk/journals
DOI: 10.1080/0144235031000075726

1. Introduction

One of the main goals in chemical physics is to understand energy transfer processes and to be able to predict the properties and dynamical behaviour of a molecular system. Van der Waals complexes constitute ideal model systems from that point of view. Because of the weakness of the intermolecular bond, the partners building the complex retain their identity and energy transfers are thus easily identified. Their dissociation represents the second half of a collision with a limited range of impact parameters, which allows one to make fruitful comparisons with collisional results. Finally, studying the dependence of the energy redistribution and fragmentation processes on the size of the cluster may help to bridge the gap with condensed-phase dynamics.

The simplest of the van der Waals complexes for studying energy transfers are built with a rare gas atom and a diatomic molecule. Among them, $Ar\cdots I_2$ has

received special attention. It exhibits very rich dynamics, with processes including vibrational predissociation (VP), intramolecular vibrational relaxation (IVR), electronic predissociation (EP) and even geminate recombination or 'caging', a typical effect usually observed in condensed phase. The interpretation of these processes has lead to many puzzles, controversies and surprises. They mainly originate from the fact that different energy transfer and decay pathways are often in competition, so that it is difficult to distinguish between them in experiments. From the theoretical point of view, competing processes should be taken into account simultaneously, which can make the problem computationally intractable. In addition, it is still nowadays quite a challenge to calculate *ab initio* the potential energy surfaces (PES)s and couplings involved in the dynamics of this system. This has made $Ar\cdots I_2$ a typical example where experiments raise a new theoretical interpretation, which is in turn tested by new experiments which can result in another interpretation, and so on until consistent and unambiguous agreement is reached. Hence $Ar\cdots I_2$ constitutes a benchmark system for comparisons between calculations and experiments.

The aim of this review is to summarize the vast amount of studies on the $Ar + I_2$ system, to identify their most important implications for the general understanding of energy transfer phenomena, to describe the current state of interpretation and controversy and to draw the perspectives for future works. We have taken the point of view of considering $Ar\cdots I_2$ as a prototypical system to study different dynamical processes, as we believe that insight gained from these studies is more general and valuable than the particular results obtained for this specific system. Therefore, the different aspects of the $Ar\cdots I_2$ structure and the various dynamical processes are discussed in separate sections, although this presentation brings some unavoidable repetitions. For the same reason, although this review is mainly devoted to the $Ar\cdots I_2$ van der Waals complex, references to other work in related fields (collisional energy transfer in the iodine molecule, caging in an inert gas matrix, structure and dynamics of related complexes, etc.) are also given when appropriate.

After a historical overview in section 2, section 3 introduces the relevant potential energy curves of the iodine molecule and details the advances made in the determination of the $Ar\cdots I_2$ interactions in the ground and excited electronic states, as well as the couplings between the electronic states of the bare molecule induced by the presence of the argon atom. Section 4 presents the cage effect in $Ar\cdots I_2$ with its different interpretations including the one now accepted, and provides a comparison with collisional recombination of I_2 and with the geminate recombination of I_2 in a solvent: large rare gas clusters, rare gas matrices, supercritical rare gases. Section 5 introduces the specific features of the VP process in $Ar\cdots I_2$, presents the different interpretations of IVR in this system and compares the behaviours of the T-shaped and linear isomers. In section 6, the origin of the EP process is discussed, as well as its possible interferences with the competing VP–IVR process. Finally, section 7 concludes and sketches perspectives for solving the open problems in this old, but still not fully understood, prototype system.

2. Historical overview

2.1. *Collisional $Ar + I_2$ system*

There is a considerable amount of literature on the collisional relaxation of excited I_2, which has been nicely summarized by Krajnovich *et al.* (1989a). The

beginning of this long history may be traced back to Wood, (1911a,b), who measured the reduction of fluorescence intensity of an I_2 cell exposed to sunlight as a function of the pressure of added gases and showed that the fluorescence spectra were gradually evolving from discrete to band spectra as the pressure of the rare gas increased in the cell (Franck and Wood 1911).

A correct interpretation of these pioneering results was not possible until the advent of quantum mechanics. It is now known that I_2 visible absorption is related to the $B(^3\Pi 0_u^+) \leftarrow X(^1\Sigma 0_g^+)$ electronic transition. Fluorescence quenching of the $I_2(B)$ excited state by foreign gases is related to electronic transitions from the B state to repulsive electronic states (see sections 3.1, 3.5 and 6) induced by interaction with a colliding atom. This leads to the fragmentation of the I_2 molecule into two hot I atoms which cannot fluoresce. The qualitative changes in the fluorescence spectra are related to vibrational and rotational transitions induced by collision between $I_2(B)$ and the foreign gas.

During several decades, experiments on the subject remained qualitative because they were recorded on photographic plates (Rössler 1935, Arnot and McDowell 1958). Quantitative fluorescence spectra of $I_2(B)$ and its quenching by Ar became possible with the advent of photomultipliers, as first obtained by Klemperer and his group (Brown and Klemperer 1964, Steinfeld and Klemperer 1965), followed by others (Kurzel and Steinfeld 1970, Capelle and Broida, 1973, Nakagawa *et al.* 1986), and became more systematic with the use of tunable laser sources (Capelle and Broida 1973, Nakagawa *et al.* 1986). The dependence of the quenching cross-section on the initial vibrational excitation v' was found to be rather smooth, with an average quenching cross-section of the order of $5\,\text{Å}^2$ (Capelle and Broida 1973). Vibrational energy transfer is more efficient as v' increased (Steinfeld and Klemperer 1965) and less efficient than rotational energy transfer (Rubinson *et al.* 1974).

Although the global picture for these phenomena is clear, a detailed theoretical interpretation of these results was slow to emerge and is still nowadays not fully satisfactory. The quenching cross-section was found to be proportional to the polarizability of the target and to the duration of the collision, and hence to the square root of the reduced mass of the system (Rössler 1935, Selwyn and Steinfeld 1969). Two independent models were developed (Selwyn and Steinfeld 1969, Thayer and Yardley 1972), based on a perturbative treatment of the instantaneous dipole–dipole interaction, but differing in the definition of the final state after quenching. According to Selwyn and Steinfeld (1969), the quencher can be in any final state, in which case the instantaneous dipole couples at the first order of perturbation theory the I_2 initial $B(^3\Pi 0_u^+)$ state with final states which have a *g* or *u* symmetry opposite to the initial one $(a\,1_g, a'\,0_g^+)$. On the other hand, Thayer and Yardley (1972) assumed similar initial and final states for the quencher, in which case the final states of I_2 must have the same *g* or *u* symmetry as the initial B state and the quenching could be attributed to the 0_u^- state (Nakagawa *et al.* 1986). This contradiction could in principle be solved by looking at the dependence of the quenching cross-section on the initial vibrational state, which is related to the Franck–Condon factors between the initial bound state and the final continuum state. Unfortunately, the quenching rate was found to be a smooth function of the initial excitation (Nakagawa *et al.* 1986, Capelle and Broida 1973). This could result from competition with collisional vibrational energy transfer (Tellinghuisen 1985). Selection of the initial state had to wait for the advent of low-temperature supersonic beams, where van der Waals complexes are formed in well-defined initial states and can undergo processes such as

VP or EP closely related to vibrational energy transfers and quenching in collisional conditions.

2.2. *The $Ar\cdots I_2$ van der Waals complex*

The first experimental evidence of the existence of the $Ar\cdots I_2$ van der Waals complex was obtained by Levy and his team (Kubiak *et al.* 1978, Levy 1981). In a series of pioneering experiments (Smalley *et al.* 1976, Kubiak *et al.* 1978, Johnson *et al.* 1978, Sharfin *et al.* 1979, Blazy *et al.* 1980, Kenny *et al.* 1980a,b, Johnson *et al.* 1981, Levy 1981), Levy and coworkers have studied the spectroscopy and dynamics of I_2 van der Waals complexes in a supersonic expansion, via the $B \leftarrow X$ transition. After a first unsuccessful attempt (Smalley *et al.* 1976), the $Ar\cdots I_2$ fluorescence excitation spectrum was observed only for vibrational levels of $I_2(B)$ higher than $v' = 12$. The laser-induced fluorescence intensity was found to be an oscillatory function of the I_2 vibrational excitation. This behaviour was interpreted as the result of the competition between VP and EP:

$$Ar\cdots I_2(B, v') \xrightarrow{VP} Ar + I_2(B, v \leq v') \quad (1)$$

$$Ar\cdots I_2(B, v') \xrightarrow{EP} Ar + I(^2P_{3/2}) + I(^2P_{3/2}). \quad (2)$$

Since channel (1) produces electronically excited I_2 fragments which can fluoresce while channel (2) is dark, measurements of the I_2 fluorescence quantum yield in conjunction with the $Ar\cdots I_2$ absorption spectrum can provide the relative importance of VP and EP. For $v' < 12$ EP dominates, which explains why no fluorescence could be detected.

Goldstein *et al.* (1986) measured the relative quantum yields for $Rg\cdots I_2$ complexes, with Rg = He, Ar, Kr and Xe. In agreement with the results of Levy and coworkers (Kubiak *et al.* 1978), they observed no significant variation of the quantum yield as a function of the excited vibrational state for $He\cdots I_2(B, v')$, while for $Ar\cdots I_2(B, v')$ an oscillatory behaviour with v' was confirmed. For $Kr\cdots I_2$ complexes the extremely low fluorescence quantum yield measured (Goldstein *et al.* 1986) indicates that the rates associated with VP and EP become comparable only for v' values close to the $I_2(B)$ dissociative threshold. For complexes of Xe or more than one Ar atom, however, no fluorescence was detected, clearly indicating that EP becomes the dominant channel. Therefore, $Ar\cdots I_2$ is an ideal system to study the competition between VP and EP. Whether the oscillations of the fluorescence intensity are due to EP or VP is still a subject of debate. A related question is whether VP dynamics, which is mediated by IVR, is in a sparse or statistical regime. Another issue is the nature of the electronic state(s) responsible for EP. These points will be discussed in sections 5 and 6.

2.3. *Cage effect*

Another puzzling effect was found in $Ar\cdots I_2$. When excited above the B state dissociation limit, complexed I_2 still exhibits some fluorescence, whereas uncomplexed I_2 is 100% dissociated at the same wavelength. This means that the presence of one sole argon atom can induce the recombination of the departing I atoms into I_2. This process is reminiscent of a well-known condensed phase process, the so-called 'cage effect'.

The condensed-phase 'cage effect' is a process in which two dissociating fragments recombine *in situ* by colliding with atoms or molecules of the surrounding solvent (the 'cage'). It is also called 'geminate recombination' as opposed to recombination after diffusion, and was introduced by Franck and Rabinovitch (1934) to explain the reduced photochemical yield of free radicals in solutions as compared with the gas phase. Since then, it has played a central role in the reactive photodynamics studies in condensed media. These include photodissociation studies of small molecules in van der Waals solids and clusters (Chergui and Schwentner 1992), in the liquid phase (Harris *et al.* 1988) and in high pressure gases (Schroeder and Troe 1987), by time-independent experiments and by molecular dynamics simulations, as well as more recent femtosecond time-resolved measurements in clusters (Papanikolas *et al.* 1992, 1993), in liquids (Alfano *et al.* 1992, Zewail *et al.* 1992, Schwartz *et al.* 1993), in high-pressure gases (Lienau and Zewail 1994) and in solids (Zadoyan *et al.* 1997, Apkarian and Schwentner 1999, Pedersen and Weitz 2002). In many of these studies, I_2 is the prototype molecule to investigate the photodissociation–recombination process.

Molecular clusters offer a unique environment to study cage effects, since the size of the solvent cage surrounding a chromophore can potentially be controlled, allowing one to study the effect of increasing solvation on reaction dynamics (Castleman 1992, Fei *et al.* 1992, Hu and Martens 1993b, Liu *et al.* 1993, Papanikolas *et al.* 1993, Gerber *et al.* 1994, Jungwirth *et al.* 1996, Greenblatt *et al.* 1997, Delaney *et al.* 1999, Žďánská *et al.* 2000, Baumfalk *et al.* 2001, Sanov and Lineberger 2002). The interpretation of the cage effect in $Ar\cdots I_2$ has led to several rebounds, from a purely kinematic or 'ballistic' to a non-adiabatic process. A major surprise came in the interpretation of a crucial experiment designed to distinguish between the possible mechanisms (Burke and Klemperer 1993b). The conclusion of that experiment was that two isomers must coexist in supersonic expansions, a perpendicular one recognized early on and a linear one that was conjectured to explain the results. Its existence was later confirmed and has led to a new series of experimental and theoretical studies to examine the dependence of the different processes on the initial geometry of the complex. The study of the cage effect in $Ar\cdots I_2$ is detailed in section 4, while a comparative study of the VP/EP fragmentation dynamics from the two isomers will be presented in section 5.

It emerges from this historical survey that although the $Ar\cdots I_2$ van der Waals complex contains only a diatomic molecule and a rare gas atom, it can be seen as a prototype to study a wide range of molecular physics processes, from VP involving complex IVR dynamics to the typical condensed-phase cage effect, through EP and its competition with IVR–VP. Also, last but not least, these processes can be studied in two different geometries, corresponding to the linear and T-shaped isomers of $Ar\cdots I_2$.

3. Structure, energetics and PESs

The range of dynamical processes present in $Ar\cdots I_2$, as well as their complexity, requires an accurate description of the $Ar–I_2$ interaction in the ground and excited electronic states of I_2, as well as that of the couplings between these states induced by the argon. This section describes and comments the various approaches that have been used until now to tackle this difficult task.

First, we briefly summarize the useful information on the structure of the isolated I_2 molecule. Second, we go into the details of the various pieces of information gained from different experimental measurements. Then the empirical, semiempirical and *ab initio* approaches to the $Ar\cdots I_2$ potentials and couplings are described.

3.1. *Electronic structure of the I_2 molecule*

The valence states of the iodine molecule form the lowest manifold of the molecular terms correlating with the $I(^2P) + I(^2P)$ dissociation limit. When spin–orbit (SO) interaction is taken into account, the asymptotic threshold splits into three limits; $I(^2P_{3/2}) + I(^2P_{3/2})$, $I(^2P_{3/2}) + I^*(^2P_{1/2})$ and $I^*(^2P_{1/2}) + I^*(^2P_{1/2})$, separated by the atomic SO splitting $A = 7602.98\,cm^{-1}$. The detailed description of the valence states for iodine goes back to the classical work of Mulliken (1957, 1971). It was shown that their structure obeys Hund's case (c) coupling scheme with Ω_w^σ classification, where Ω is the projection of the total (orbital plus spin) electronic angular momentum on the I_2 axis **r**, $\sigma = \pm 1$ and $w = u, g$ being the parities with respect to coordinate inversion (reflection of the electronic coordinates through the a plane containing the molecular axis) and nuclear permutation (inversion of electronic coordinates in the body-fixed frame) respectively.

The valence manifold consists of 23 levels (36 states, 13 levels being doubly degenerate), namely, $X\,0_g^+$, $a'\,0_g^+$, $3\,0_g^+$, $4\,0_g^+$, 0_g^-, $B\,0_u^+$, $B'\,0_u^-$, $2\,0_u^-$, $3\,0_u^-$, $4\,0_u^-$, $a\,1_g$, $2\,1_g$, $3\,1_g$, $A\,1_u$, $B''\,1_u$, $3\,1_u$, $4\,1_u$, $5\,1_u$, $1\,2_g$, $2\,2_g$, $A'\,2_u$, $2\,2_u$, and 3_u, where the most common spectroscopic notations for iodine are used (Huber and Herzberg 1979).

They originate from 12 non-relativistic precursors in Hund's case (a) $^{2S+1}\Lambda_w^\sigma$ classification (where Λ is the projection on the molecular axis of the electronic orbital angular momentum and Σ is the spin angular momentum) $1\,^1\Sigma_g^+$ $(X\,0_g^+)$, $2\,^1\Sigma_g^+$ $(4\,0_g^+)$, $^1\Sigma_u^-$ $(3\,0_u^-)$, $^1\Pi_g$ $(2\,1_g)$, $^1\Pi_u$ $(B''\,1_u)$, $^1\Delta_g$ $(2\,2_g)$, $^3\Sigma_g^-$ $(3\,0_g^+, 3\,1_g)$, $1\,^3\Sigma_u^+$ $(2\,0_u^-$, $C\,1_u)$, $2\,^3\Sigma_u^+$ $(4\,1_u, 4\,0_u^-)$, $^3\Pi_g$ $(1\,2_g, a\,1_g, 0_g^-, a'\,0_g^+)$, $^3\Pi_u$ $(A'\,2_u, A\,1_u, B'\,0_u^-, B\,0_u^+)$, and $^3\Delta_u$ $(3_u, 2\,2_u, 5\,1_u)$.

The literature provides a wealth of information on the valence potential energy curves. Empirical curves are available for 10 of these states (for a brief account see, for example, Buchachenko and Stepanov, (1996b) and Pazyuk *et al.* (2001)). In addition, two high-level relativistic *ab initio* calculations on the complete set of I_2 electronic states have been performed (Teichteil and Pélissier 1994, de Jong *et al.* 1997).

Since the $X(^1\Sigma\,0_g^+)$ and $B(^3\Pi 0_u^+)$ states are of prime interest in the present context, it is worth referring to the accurate empirical Rydberg–Klein–Rees potential curves (Martin *et al.* 1986, Gerstenkorn and Luc 1985). The B state correlates with the $I + I^*$ asymptotic limit and intersects repulsive or weakly bound electronic states $(B''\,1_u,\ 1\,2_g,\ a\,1_g,\ a'\,0_g^+\ 2\,0_u^-$ and $3_u)$ going to the ground $I + I$ asymptote, as illustrated in figure 1. These states are responsible for various EP processes of $I_2(B)$ (Katô and Baba 1995), which are very slow in isolated I_2.

Above the valence states there is a manifold of so-called ion-pair states correlating with the $I^+(^3P_j, ^1D_j) + I^-(^1S_0)$ dissociation limits.

3.2. *$Ar\cdots I_2(X,B)$ dissociation energies: The existence of two isomers*

The initial studies on vibrationally inelastic $Ar + I_2$ collisions did not bring any direct, accurate information on the Ar–I_2 interaction. Real progress was made in the late 1970s by Levy and coworkers in their spectroscopic investigations of van der Waals $Rg\cdots I_2$ complexes in a supersonic expansion via the $B(^3\Pi\,0_u^+) \leftarrow X(^1\Sigma\,0_g^+)$

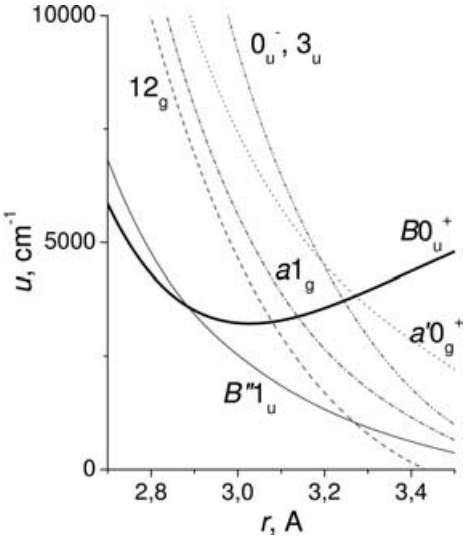

Figure 1. Potential energy curves of the B and crossing valence states of molecular iodine. The zero for energies is the lowest $I(^2P_{3/2}) + I(^2P_{3/2})$ dissociation limit.

transition (Smalley *et al.* 1976, Kubiak *et al.* 1978, Sharfin *et al.* 1979, Blazy *et al.* 1980, Kenny *et al.* 1980a, Johnson *et al.* 1981, Levy, 1981); see section 2. Excitation spectroscopy was supplemented by dispersed fluorescence measurements which probed the final vibrational state distribution v of the VP products (Blazy *et al.* 1980). For excitations to $v' < 30$, VP proceeds through the transfer of $\Delta v = v' - v = -3$ quanta. For $v' = 30$, the $\Delta v = -3$ product disappears and VP proceeds through the transfer of four vibrational quanta, owing to the anharmonicity of the I_2 vibration which reduces the vibrational quantum energy when v increases. This allowed Blazy *et al.* (1980) to establish firmly both upper and lower limits for D_0 of $Ar\cdots I_2$: $D_0(B) = 223 \pm 3\,cm^{-1}$. The detection of additional spectral bands assigned to B state excited van der Waals levels (intermolecular stretching and double bending excitation) made it possible to estimate the vibrational frequencies and zero-point energy and to deduce the binding energy $D_e(B)$. The dissociation energy in the X state was determined from the (blue) frequency shift of the complexed versus uncomplexed I_2 transition: $D_0(X) = 237 \pm 3\,cm^{-1}$. The estimations for binding energies are collected in tables 1 and 2.

At the time at which these results were obtained, there was no definitive structural information available for the $Ar\cdots I_2$ complex. $Ar\cdots ClF$ was known to be linear from microwave studies (Harris *et al.* 1974). However, the structure of $He\cdots I_2$ had been determined by Levy and coworkers (Smalley *et al.* 1978) to be T shaped from analysis of rotationally resolved bands of the $B \leftarrow X$ transitions. The smaller rotational constants of $Ar\cdots I_2$ did not allow the same level of resolution, but it was assumed to be T shaped by analogy with $He\cdots I_2$. This geometry was given even more credit by subsequent studies of dihalogen–rare gas complexes characterized to be T shaped from rotational analysis of the $B \leftarrow X$ transition, e.g. $Ne\cdots Br_2$ (Thommen *et al.* 1985), $Ne\cdots Cl_2$ (Evard *et al.* 1986) and $Ar\cdots Cl_2$ (Evard *et al.* 1988b), and from the microwave spectroscopy of $Ar\cdots Cl_2(X)$ (Xu *et al.* 1993). It was later confirmed by Burke and Klemperer (1993a) that the $B \leftarrow X$ spectrum could be fitted using a perpendicular geometry for $Ar\cdots I_2$.

Table 1. Equilibrium distances R_e (Å) and binding energies D_e (cm^{-1}) of the T-shaped and linear minima for selected $Ar\cdots I_2$ PESs of the X and B electronic states. For experimental data from Levy's and Klemperer's groups (cited as Levy and Klemperer), approximate estimations of D_e from D_0 are given with the error bars of the D_0 values. PP stands for pairwise potential.

			T shaped		Linear	
Entry	State	Potential or data	R_e	D_e	R_e	D_e
1	X	PP from Rg–Rg′ interaction (Secrest and Eastes 1972)	4.52	362.8	–	–
2	X	Naumkin–Knowles DIM PT1 (Naumkin and Knowles 1995)	3.93	230.1	5.31	209.6
3	X	IDIM (Buchachenko and Stepanov 1996b)	3.88	254.6	–	–
4	X	IDIM PT1 (Buchachenko and Stepanov 1996b)	3.88	254.5	–	–
5	X	DIM (Naumkin 1998)	3.93	230.5	5.13	209.5
6	X	DIM PT1 (TP2) (Buchachenko *et al.* 2000b)	3.93	233.1	5.19	189.0
7	X	DIM PT1 (dJVN2) (Buchachenko *et al.* 2000b)	3.94	230.2	5.15	201.9
8	X	*Ab initio* MP2 (Kunz *et al.* 1998)	3.95	234.4	5.12	256.7
9	X	*Ab initio* MP4 (Kunz *et al.* 1998)	4.14	187.4	5.15	205.8
10	X	*Ab initio* CCSD(T) (Kunz *et al.* 1998)	4.16	179.2	5.16	192.5
11	X	*Ab initio* CCSD-T (Naumkin and McCourt 1998c)	4.22	143.4	5.32	151.5
12	X	*Ab initio* CCSD-T RECP (Naumkin 2001)	4.02	203.1	5.09	244.4
13	X	*Ab initio* CCSD(T) RECP (Prosmiti *et al.* 2002b)	3.96	235.4	5.05	268.3
14	X	Experimental, Levy (Blazy *et al.* 1980)	–	250 ± 3	–	–
15	X	Experimental, Klemperer (Stevens Miller *et al.* 1999)	4.0 ± 0.4	166 ± 15	–	196 ± 15
16	B	PP, collision data (Rubinson *et al.* 1974)	4.24	223.8	–	–
17	B	Empirical PP (Beswick and Jortner 1978b)	3.93	200.0	–	–
18	B	PP, spectroscopic data (Gray 1992)	3.92	244.0	–	–
19	B	IDIM (Buchachenko and Stepanov 1996b)	3.83	248.8	–	–
20	B	IDIM PT1 (Buchachenko and Stepanov 1996b)	3.82	248.9	–	–
21	B	DIM (Naumkin 1998)	3.82	248.0	5.54	144.7
22	X	Experimental, Levy (Blazy *et al.* 1980)	–	236 ± 3	–	–
23	X	Experimental, Klemperer (Stevens Miller *et al.* 1999)	–	140 ± 15	–	–

The first accurate large-scale *ab initio* calculations performed for $Ar\cdots Cl_2(X)$ by Tao and Klemperer (1992) gave a quite unexpected result: two minima were found, a T-shaped and a linear one, the latter being significantly deeper. This could be rationalized in the following manner. In the X state the σ^* orbital of a dihalogen molecule is empty, which may result in a fairly short equilibrium bond length and hence a stronger binding energy for the linear isomer. This finding was later confirmed by numerous *ab initio* studies of the ground-state chlorine and bromine complexes (Chałasiński *et al.* 1994, Naumkin and Knowles 1995, Naumkin and McCourt 1997, Rohrbacher *et al.* 1997a, Williams *et al.* 1997, Naumkin and McCourt 1998a, Rohrbacher *et al.* 1999a,b, Cybulski and Holt 1999, Naumkin and McCourt 1999, Prosmiti *et al.* 2002a) and seemed to be in contradiction with experiment, which only detected T-shaped isomers.

Table 2. Dissociation energies D_e and D_0 (cm^{-1}) of the T-shaped and linear isomers of the $Ar\cdots I_2(X, B)$ complex from experimental data and selected PESs.

			T-shaped		Linear	
State	Potential or data	Reference	D_e	D_0	D_e	D_0
X	DIM PT1	Buchachenko *et al.* (2000b)	233	209	189	166
X	CCSDT(T) RECP	Prosmiti *et al.* (2002b)	235	212	268	238
X	Levy, experiment	Blazy *et al.* (1980)	250	237 ± 3	—	—
X	Klemperer, experiment	Stevens Miller *et al.* (1999)	166	142 ± 15	196	172 ± 1.5
B	DIM PT1	Buchachenko and Stepanov (1996b)	249	222	—	—
B	Gray's PP	Gray (1992)	244	222	—	—
B	Levy, experiment	Blazy *et al.* (1980)	236	223 ± 3	—	—
B	Klemperer, experiment	Stevens Miller *et al.* (1999)	140	128 ± 15	—	—

This contradiction was solved by Huang *et al.* (1995) for $He\cdots Cl_2$. These authors demonstrated that the higher zero-point energy of the linear complex resulting from the doubly degenerate bending mode reversed the order of stability of the potential minima. Also, *ab initio* calculations on the B state PES (Chałasiński *et al.* 1994, Cybulski *et al.* 1995, Rohrbacher *et al.* 1997b, Williams *et al.* 1999) proved that its minimum is T shaped and that transitions from the ground-state linear isomer may fall in a continuum which could go unnoticed. Indeed, on excitation to the B state, a π^* electron of I_2 is transferred to the σ^* orbital, thus increasing the bond length and lowering the binding energy in the linear configuration. The situation in heavier complexes is less certain, mainly because of the lack of rotational resolution in experimental spectra. There are strong indications that high-resolution spectra reveal the existence of linear isomers of $He\cdots Br_2(X)$ and $Ne\cdots I_2(X)$ (Hernández *et al.* 2000, Burroughs *et al.* 2001, Buchachenko *et al.* 2002).

The first experimental evidence for the existence of a linear $Ar\cdots I_2$ isomer was obtained by Burke and Klemperer (1993b). Using $B \leftarrow X$ fluorescence excitation spectroscopy they found that the quasi-discrete spectrum observed by Levy and coworkers (Blazy *et al.* 1980, Johnson *et al.* 1981) lay on the background of a quite intense continuous absorption. Quantitative measurements of the fluorescence quantum yield were carried out for the continuum part of the absorption (Burke and Klemperer 1993b), to discriminate between two possible interpretations of the cage effect (see section 4). Burke and Klemperer concluded that the continuous absorption was due to a linear isomer which coexisted in the jet with the T-shaped one, with a population ratio estimated to be 3:1 (Burke and Klemperer 1993b).

More evidence in support of this interpretation came from *ab initio* calculations discussed in section 3.6 and from experiments by the group of Donovan and Lawley (Cockett *et al.* 1993, 1994, Goode *et al.* 1994, Cockett *et al.* 1996) on the high-lying Rydberg states of the $Ar\cdots I_2$ complex. Many of the vibrational bands in the resonance-enhanced multiphoton ionization and zero electron kinetic energy (ZEKE) spectra of the Rydberg states converging to the ground state of the complex cation were split into doublets (Cockett *et al.* 1993, 1994), subsequently assigned (Cockerr *et al.* 1996) to transitions from the T-shaped and linear isomers.

Measurements of the vibrational distributions of the photofragmentation products allowed Stevens Miller (1999) to determine the dissociation energy of the linear $Ar\cdots I_2(X)$ isomer as $D_0(L,X) = 172 \pm 4\,cm^{-1}$. From their previous estimate of a 3:1 linear:T-shaped isomer population based on intensity measurements, these authors concluded that the linear isomer should be more stable than the T-shaped one by *ca.* $30\,cm^{-1}$, assuming thermal equilibrium at a temperature of $15 \pm 5\,K$. This yielded a dissociation energy for the latter of $D_0(T,X) = 142 \pm 15\,cm^{-1}$, and hence of $D_0(T,B) = 128 \pm 15\,cm^{-1}$ for the excited state (Stevens Miller *et al.* 1999). These results contradict the determination of $D_0(T,B) = 223 \pm 3\,cm^{-1}$ by Levy's group (Blazy *et al.* 1980). Indeed, if the revised B state dissociation energy is correct, the $\Delta v = -2$ VP channel should be open and dominant. Klemperer and coworkers suggested that the $\Delta v = -2$ channel could have been present in Levy's experiment but not detected. This could be because $\Delta v = -2$ VP fragments are slow to separate since translational energy is very low for that channel, and fluorescence from $I_2(v' - 2)$ could be quenched by the competing EP process. Photofragmentation of the linear isomer is much faster, so that the corresponding vibrational product state distributions are unlikely to be affected by EP.

The value of $D_0(T,X)$ determined by anion photoelectron spectroscopy of $Ar\cdots I_2^-$ (Asmis *et al.* 1998) combined with the available estimation of $Ar\cdots I_2^-$ dissociation energy (Naumkin and McCourt 1999), $D_0(T,X) = 190 \pm 80\,cm^{-1}$, did not resolve the controversy on $Ar\cdots I_2$ energetics, since the error bars cover both Levy's and Klemperer's values.

In order to resolve this contradiction, Burroughs and Heaven (2001) implemented the optical–optical double-resonance technique to measure the rotational j distributions of the $I_2(B)$ fragment after excitation of both the T-shaped and the linear isomers. The value $220\,cm^{-1} \leq D_0(T,B) \leq 232\,cm^{-1}$ was deduced from energy conservation at the highest value of j observed, in perfect agreement with the result of Levy's group. These observations cannot completely rule out the assumption of Klemperer *et al.* since higher rotational channels could also be quenched by EP, but the similarity of the $D_0(T,B)$ values adds more arguments in support of Levy's data.

Burroughs and Heaven (2001) suggested that another weak point in the deduction of the dissociation energies from intensity measurements was the assumption of thermal equilibrium in the beam. This point has been the subject of a thorough molecular dynamics simulation (Bastida *et al.* 2002) describing the collisional isomerization and cooling of $Ar\cdots I_2(X)$ in a free jet using the CCSD(T) PESs by Kunz *et al.* (1998) described in section 3.6. This simulation has reached the surprising conclusion that the populations of the two isomers remain in thermal equilibrium as the expansion proceeds. This is because, when an argon atom enters the potential well of an already formed $Ar\cdots I_2$ complex, it acquires a kinetic energy much larger than its asymptotic value, which can make the complex overcome its isomerization barrier. Another mechanism was also put in evidence, in which a linearly incoming argon atom could replace the perpendicularly attached atom or vice versa, the net effect being isomerization with the exchange of argon atoms: this mechanism was called 'swap cooling' and could account for up to half of the coldest collisions.

Other possible sources of inaccuracy affecting the derivation of $D_0(T,X)$ are probably related to intensity ratio determination, namely the problem of distinguishing the absorption from each isomer, different absorption probabilities and the

possible role of saturation effects (Klemperer 2001). We come back to this point in section 5.3.

3.3. *Empirical potentials*

Initially, the need for Ar–I_2(X,B) interaction potentials arose from experiments on vibrationally inelastic collisions (e.g. Brown and Klemperer 1964, Steinfeld and Klemperer 1965, Kurzel and Steinfeld 1970, Kurzel *et al.* 1971, and the literature database in Steinfeld 1984, 1987). These measurements performed under bulk conditions provided estimations for inelastic transition rate constants which do not allow straightforward inversion of the potential. Early theoretical interpretations (Kajimoto and Fueno 1972, Rubinson *et al.* 1974, Rubinson and Steinfeld 1974) designed and used empirical potentials representing the total PES as a sum of atom–atom potentials (Hill 1946, Kitaigorodskii 1951). The addition of two identical potentials gives a PES with a T-shaped configuration and a saddle point in the collinear arrangement. The Rg–X rare gas–halogen potentials were approximated by Rg–Rg′ potentials from Hirschfelder *et al.* (1954), where Rg′ is the rare gas atom following X in the periodic table (see, for example, the work by Secrest and Eastes (1972)) or by simple correlation rules.

A notable exception is the work of Rubinson *et al.* (1974), where the parameters of a model Buckingham Rg–I potential were optimized by means of three-dimensional quasi-classical trajectory calculations to reproduce observed probabilities of vibrationally inelastic transitions in $Rg + I_2(B)$ collisions. Equilibrium properties of these potentials are presented in table 1 entry 16.

Later, more collision experiments were carried on the vibrationally (Sulkes *et al.* 1980, Hall *et al.* 1983, Gentry 1984, Baba and Sakurai 1985, Rock *et al.* 1988, Krajnovich *et al.* 1989a,b, Du *et al.* 1991, Ma *et al.* 1991, Nowlin and Heaven 1993, Lawrence *et al.* 1997) and rotationally (Dexheimer *et al.* 1982, 1983, Derouard and Sadeghi 1984a,b,) inelastic scattering, collisional line broadening (Drabe *et al.* 1985b,a, Drabe and van Voorst 1985) and diffusion coefficients (Starovoitov 1990, Gardner and Preston 1992) of the iodine molecule, but none of them contributed to the determination or refinement of $Ar \cdots I_2$ PES.

The first pioneering theoretical studies (Beswick and Jortner 1978b,a) on the $Ar \cdots I_2$ van der Waals complex used model pairwise Morse potentials very convenient for analytical studies (table 1, entry 17). These and further work (Ewing 1979, Beswick and Jortner 1980, Ewing 1980, 1982, Halberstadt and Beswick 1982, Ewing 1986, Kokubo and Fujimura 1986, Gray *et al.* 1986, Gray and Rice 1986, Zhao and Rice 1992, Buchachenko and Stepanov 1993) contributed a lot to the development of the theoretical formalism and the qualitative understanding of the VP dynamics, but not to the improvement of interaction PESs.

The most realistic empirical $Ar \cdots I_2$(B) PES was suggested by Gray (1992) as a sum of pairwise Morse interactions (table 1, entry 18) on the basis of experimental data by Blazy *et al.* (1980) and correlations with structural parameters of $Ar \cdots Cl_2$. This PES has been used in many thorough studies of $Ar \cdots I_2$(B) dynamics (Gray 1992, Roncero *et al.* 1994b, Roncero and Gray 1996, Roncero *et al.* 1996, Bastida *et al.* 1997, Goldfield and Gray 1997b, Bastida *et al.* 1999).

For completeness, a few words should be said about other empirical potentials implemented in the studies of large clusters and condensed phases. Most such work (e.g. Borrmann and Martens 1993, Hu and Martens 1993a, Zadoyan *et al.* 1994a,b, Ben-Nun *et al.* 1995, Li *et al.* 1995, Liu *et al.* 1995, Liu and Guo 1995, Schek *et al.*

1996) used simple Lennard-Jones pair potentials, common and convenient in molecular dynamics and Monte Carlo simulations. In their study of the cage effect in $Ar_n\cdots I_2$ clusters, Schröder and Gabriel (1996) derived a set of pairwise Morse potentials with a modified long-range part. Like Gray's curves, they were parametrized mainly by using the experimental data of Blazy *et al.* (1980).

3.4. *Diatomics-in-molecule models*

Diatomics-in-molecule (DIM) based models, which provide a way for constructing the PESs of a polyatomic molecule from the electronic properties of its diatomic fragments (Tully 1977, Kuntz 1979, 1982), appear to be very popular and useful for studying the $Rg\cdots X_2$ complexes. Different approaches applied to these systems, primarily $He\cdots Cl_2$ and $Ar\cdots I_2$, provide not only a route for improving the accuracy of results but also a qualitative insight into the importance of various factors governing their electronic structure. For completeness, we present in appendix 1 a brief description of the particular DIM-based approach which covers and classifies all the models used so far for $Ar\cdots I_2$.

In many cases, application of the DIM methodology to weakly bound systems is hampered by the lack of reliable potentials for diatomic fragments. Fortunately, it is not the case for $Rg\cdots X_2$ complexes. Analysis of molecular beam scattering data (Becker *et al.* 1979, Casavecchia *et al.* 1982, Aquilanti *et al.* 1988, 1990, 1993), ZEKE photoelectron spectroscopy of $Rg\cdots X^-$ anions (Zhao *et al.* 1994, Yourshaw *et al.* 1996, 1998, Lenzer *et al.* 1998, 1999) and high-level *ab initio* calculations (Burcl *et al.* 1998, Lara-Castells *et al.* 2001, Buchachenko *et al.* 2001, Partridge *et al.* 2001) provided very accurate fragment interaction potentials. In the case of $Ar\cdots I$, the most accurate potentials originate from ZEKE measurements (Zhao *et al.* 1994, Yourshaw *et al.* 1996) They are used in all DIM applications to $Ar\cdots I_2$.

The first implementation of the DIM approach to a $Rg\cdots X_2$ system was made by Gersonde and Gabriel (1993), who investigated Cl_2 photodissociation in solid Xe. They used the complete DIM method in the non-relativistic version (I_2 eigenstates were taken as pure Hund's case (a) r-independent functions, where r stands for the I_2 bond length), and the non-diagonal diabatic couplings between the I_2 states of the same symmetry (two 2×2 blocks of $^1\Sigma_g^+$ and $^3\Sigma_u^+$ symmetry, see section 3.1) were ignored.

Two years later, Naumkin and Knowles (1995) proposed a simple analytical formula to describe the ground-state interaction PES of $Rg\cdots X_2$ complexes:

$$U_X = \sum_{\alpha=a,b} \left(V_\Sigma^\alpha \cos^2\beta_\alpha + V_\Pi^\alpha \sin^2\beta_\alpha\right), \tag{3}$$

where, for brevity, $V_\Lambda^\alpha = V_\Lambda(\mathcal{R}_\alpha)$ is the potential of the Rg–X molecule in its $\lambda = 0$ (Σ), ± 1 (Π) state as a function of the X_α–Rg distance $\mathcal{R}_\alpha$, and β_α is the angle between the $\mathcal{R}_\alpha$ vector and the I_2 axis (see appendix 1). This elegant formula corresponds to a diagonal element of the complete DIM Hamiltonian matrix of Gersonde and Gabriel (Buchachenko and Stepanov 1997a). For $Ar\cdots I_2$ it gives a PES with two minima in the T-shaped and linear configurations with well depths $D_e(T,X) = 230\,cm^{-1}$ and $D_e(L,X) = 210\,cm^{-1}$ (table 1, entry 2). This model predicts a similar topology for the PESs of other $Rg\cdots X_2(X)$ systems (Naumkin and McCourt 1997, 1998a, 1999). It was proven to be very efficient in combination

with *ab initio* calculations when true Rg–X interaction potentials are replaced by effective ones.

Soon after, another DIM-based model was suggested for $Ar\cdots I_2$ (Buchachenko and Stepanov 1996b) (its almost exact analogue was independently developed and used for simulations of I_2 photodynamics in condensed rare gases by Batista and Coker (1996)). The electronic wavefunctions of the bare I_2 molecule (solutions of the Schrödinger equations for $\hat{H}_0$, see equations (11) and (14) of appendix 1) were approximated by expansions over products of coupled Hund's case (c) $|jm\rangle$ atomic functions with coefficients (the $C_k^n(r)$ in equation (15) of appendix 1) frozen at their asymptotic ($r \to \infty$) value. Because this approximation neglects a significant part of intramolecular interactions in the halogen molecule, it was called the intermolecular DIM (IDIM) model. Its accuracy depends on the state considered. It is certainly valid for the $B(^3\Pi\, 0_u^+)$ state which is the unique valence state in its symmetry representation. It is more questionable if there are several states of the same symmetry, as for the $X(^1\Sigma\, 0_g^+)$ state, since the exact wavefunction should then be represented as an r-dependent linear combination of asymptotic solutions. For instance, the IDIM model gives a single T-shaped minimum with $D_e = 249\,cm^{-1}$ (table 1, entry 19) for the B state, in very good agreement with the experimental data (Blazy *et al.* 1980) and with the best empirical PES (Gray 1992). The corresponding dissociation energy $D_0(B) = 222\,cm^{-1}$ falls within the error bars of the experimental estimation by Blazy *et al.* (1980). The corresponding PES for the ground state (table 1, entry 3) also agrees well with Levy's data for $D_0(T, X)$, but it does not exhibit a minimum in the linear configuration.

The approximation which treats the Ar–I_2 interaction (the $\hat{H}_1$ term in equation (12) of appendix 1) as a first-order perturbation to the sum of monomer Hamiltonians ($\hat{H}_0$ in equation (11) of appendix 1) is called the IDIM PT1 approximation (perturbation theory first order). An attractive feature of this approximation is that all the electronic properties can be expressed in an analytical form (Buchachenko and Stepanov 1997a, 1998a). In particular, the following simple formula for the B state PES was derived:

$$U_B = \frac{1}{4}\sum_{\alpha=a,b}\left[3V_\Sigma^\alpha + V_\Pi^\alpha - (V_\Sigma^\alpha - V_\Pi^\alpha)\cos^2\beta_\alpha\right]. \tag{4}$$

This approach has been applied to several $Rg\cdots X_2(B)$ complexes, namely, $He\cdots Cl_2$ (Grigerenko *et al.* 1997b, Buchachenko and Stepanov 1998b), $Ne\cdots Cl_2$ (Buchachenko and Stepanov 1997b), $Ar\cdots Cl_2$ (Buchachenkon and Stepanov 1996a), $He\cdots Br_2$ (Buchachenko *et al.* 2000a, Hernández *et al.* 2000, Buchachenko *et al.* 2002), and in all cases very good agreement with experimental data on the $B(^3\Pi\, 0_u^+) \leftarrow X(^1\Sigma\, 0_g^+)$ spectra and B state VP dynamics has been obtained. Comparison between the IDIM and IDIM PT1 minima of the B state presented in table 1 indicates the validity of the first-order perturbative approximation.

Grigorenko *et al.* (1997b) published the results of a thorough DIM investigation of the $He\cdots Cl_2$ electronic structure and showed that proper inclusion of the diabatic coupling matrix elements between the non-relativistic X_2 electronic states of the same symmetry is necessary. For $Ar\cdots I_2$, a similar DIM approach was implemented by Naumkin (1998) but using Cartesian orbitals as atomic functions. With this choice, the diabatic couplings between the states of the same symmetry are implicitly included in a rather approximate manner (Pazyuk *et al.* 2001). As a result, the

non-relativistic DIM method confirmed the Naumkin–Knowles model (equation (3)); see table 1, entry 5. It was also concluded that inclusion of SO coupling does not alter the ground-state PES, but this finding may be subject to inaccuracy since the angular transformation from the $\mathcal{R}_\alpha$ to the **r** frame (see appendix 1) is applied only to the spatial part of the atomic basis functions, not to the spin one. The results for the B state appeared to be similar to the IDIM PT1 data from equation (4) except for the existence of a shallow linear minimum at long interfragment distances; cf. entries 19–21 in table 1.

In the DIM studies reviewed above, the direct method for solving the X_2 electronic structure problem was implemented. In other words, the $\hat{H}_0$ matrix was parametrized by the non-relativistic X_2 curves taken from *ab initio* calculations. This gives rise to difficulties related to the diabatization of the 2×2 blocks of $^1\Sigma_g^+$ and $^3\Sigma_u^+$ symmetries owing to the lack of *ab initio* data. In addition, it also prevents the use of more accurate empirical information on the relativistic potential curves. To avoid these problems, the inverse method was applied by Pazyuk *et al.* (2001). The non-relativistic parameters of the $\hat{H}_0$ matrix, both energies and diabatic couplings, are adjusted to reproduce (in a least-squares sense) the full set of the true relativistic energy curves of the molecule after diagonalization. The eigenvectors obtained are then used (equations (15) and (16) of appendix 1) to construct analytical expressions for the PES and couplings, within the refined first-order perturbation theory (DIM PT1) approach. The results give a global minimum in the T-shaped geometry and a secondary minimum in the linear configuration for the X state PES and again the simple analytical formula of equation (4) for the B state. Table 1 presents the minima of the PESs obtained using two different sets of relativistic I_2 curves, TP2 (entry 6, available empirical curves plus *ab initio* curves from Teichteil and Pélissier (1994)) and dJVN2 (entry 7, same as TP2 but *ab initio* curves from de Jong *et al.* (1997)), and figure 2 presents the contour plots for the TP2 potential. The detailed analysis of the DIM PT1 results and comparison with other DIM models for $Ar\cdots I_2(X)$ can be found in Buchachenko *et al.* (2000b).

For completeness, one should also mention the very simple model $Ar\cdots I_2$ PES constructed from true Ar–I potentials (e.g. Fang and Martens 1996, Conley *et al.* 1997, Meier 1998). Although they do have some physical background, they are of course much less accurate than the PES available from the best DIM methods.

To conclude, the DIM approach provides a theoretically grounded and simple analytical interaction PES for the B state; equation (4). The best results for the X state PES obtained within the DIM PT1 model are in qualitative agreement with directly determined dissociation energies for both the linear (Stevens Miller *et al.* 1999) and the T-shaped (Blazy *et al.* 1980) isomer, with an error of the order of $30\,\mathrm{cm}^{-1}$.

3.5. *Diabatic PESs and couplings for EP dynamics*

In order to understand the dynamics of the $Ar\cdots I_2$ EP, it is necessary to know the interaction PES for six crossing states (namely, $B''\,1_u$, $1\,2_g$, $a'\,0_g^+$, $a\,1_g$, $2\,0_u^-$, and 3_u; see section 3.1) and their coupling with the $B(^3\Pi\,0_u^+)$ state, preferably in the diabatic representation. The lack of direct experimental information and of a clear interpretation of the EP process strongly limited the possibility of an empirical approach. Under the commonly accepted assumption of a $B(^3\Pi\,0_g^+) - a\,1_g$ EP mechanism, a quite realistic approximation of the corresponding diabatic coupling was derived using the long-range multipole expansion of the electrostatic interaction

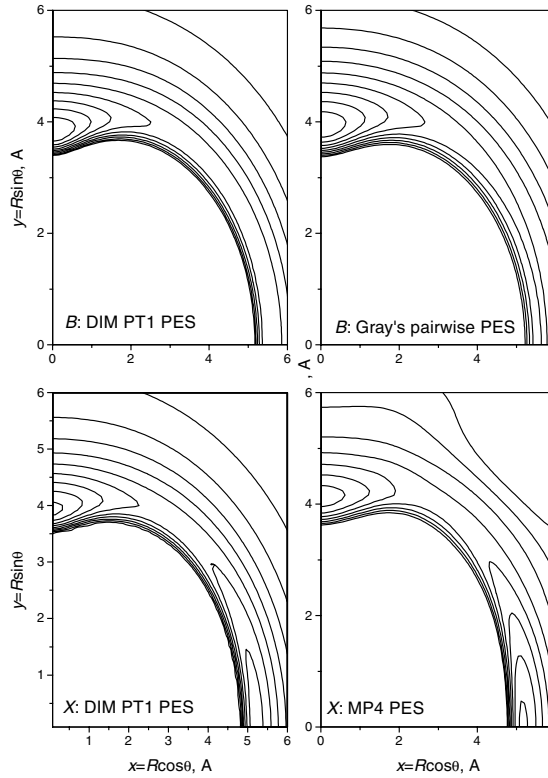

Figure 2. Contour plots of the X and B PESs of the $Ar\cdots I_2$ complex at equilibrium I—I distance. The origin is at the center of the I—I bond and the I–I vector lies along the abscissa axis. x and y are the Cartesian coordinates of the argon atom in this molecular frame. Left column: DIM PT1 (TP2) potentials for the X and B states. Right column: *ab initio* X potential and empirical B potential. Ten contour lines are equally spaced from -200 to 0 cm^{-1}.

(Roncero *et al.* 1996). However, this problem was first considered in its full complexity within the IDIM model. The topology of the PES for all crossing states was investigated. All of them have an attractive $Ar–I_2$ interaction similar to those of the X and B states. Their couplings with the B state were investigated by analysing the contribution of the different states to the adiabatic B state wavefunction (Buchachenko and Stepanov 1996b) (the presentation of the corresponding results originally contained errors and is corrected in an erratum (Buchachenko and Stepanov 1997b). The results were analysed in terms of a simple symmetry model. In brief, treating the total electronic angular momentum as the orbital one, Hund's case (c) states of I_2 can be approximately classified by irreducible representations of the $D_{\infty h}$ point group. Reduction of this group to groups describing different configurations of the complex gives the symmetry correlations presented in table 3. The states which are effectively coupled to the B state according to the IDIM model are marked by an asterisk. Table 3 also indicates that in the T-shaped configuration of the complex EP can occur only through the $a\,1_g$ state, whereas in the linear configuration it can only occur through the $a'\,0_g^+$ state. The first finding supports the EP mechanism deduced from an empirical approach (see section 6) and from a golden rule wavepacket treatment (Roncero *et al.* 1994b, 1996) which showed that

Table 3. Symmetry correlations for the B($^3\Pi\,0_u^+$) and crossing states of the I_2 molecule and the Ar · · · I_2 complex in the linear ($C_{\infty v}$), T-shaped (C_{2v}) and bent (C_s) configurations. Asterisks indicate the crossing states coupled to B within the IDIM model.

	I_2 molecule		Ar · · · I_2 complex		
State	Ω_w^σ	$D_{\infty h}$	$C_{\infty v}$	C_{2v}	C_s
B	0_u^+	Σ_u^+	Σ^+	B_2	A'
B″	1_u	Π_u	Π	$A_1 \oplus B_2$	$A'' \oplus A'^*$
a	1_g	Π_g	Π	$A_2 \oplus B_2^*$	$A'' \oplus A'^*$
a′	0_g^+	Σ_g^+	Σ^{+*}	A_1	A'^*
	3_u	Φ_u	Φ	$A_1 \oplus B_1$	$A'' \oplus A'^*$
1	2_g	Δ_g	Δ	$A_1 \oplus B_1$	$A'' \oplus A'^*$
	0_u^-	Σ_u^-	Σ^-	A_2	A''

the a 1_g and not the B″ 1_u could be responsible for the EP process. However, it will be shown in section 6 that there are more states which can effectively predissociate the B state for a given isomer than predicted from its equilibrium configuration, for dynamical reasons.

In the frame of the IDIM PT1 model, analytical formulae for the diabatic PES and coupling matrix elements can be obtained (Buchachenko and Stepanov 1998, Buchachenko 1998). The symmetry properties of the coupling functions are the same as in the complete IDIM treatment. The only exception is the 3_u state, for which the coupling to the B state is predicted to be zero by IDIM PT1 and is found to be very weak (probably reflecting second-order interactions) in the IDIM approach.

The most accurate data on the PES and couplings for the crossing states have been obtained using the DIM PT1 model from Buchachenko *et al*. (2000b). They are briefly described in Lepetit *et al*. (2002). Figure 3 shows the contour plots of the non-vanishing B state couplings with the B″1_u, $1\,2_g$, a′0_g^+ and a 1_g states. The refined DIM PT1 approach does not alter the symmetry properties of the couplings and hence the important qualitative propensities to predissociate electronically through the a 1_g and a′0_g^+ states for the T-shaped and linear isomers respectively.

3.6. Ab initio *calculations*

The first *ab initio* calculations on the Ar · · · I_2(X) PES were performed in 1998 by Kunz *et al*. (1998) who used a variety of extended atomic orbital (AO) basis sets and the methods of correlation treatment. Studying the electronic structure of the Ar · · · I and I_2 fragments, these authors concluded that within an all-electron treatment the SO interaction should not be essential for the interaction PES. Their best results were obtained at the non-relativistic coupled cluster CCSD(T) (coupled cluster expansion including single and double excitations with non-iterative correction to triple excitations) level of theory. They are presented in table 1 (entry 10) together with less accurate data by second- and fourth-order Møller-Plesset perturbation theory (MP2 and MP4, entries 8 and 9). The results vary depending on the method, but the essential features of the PES—a global minimum at the linear geometry and a secondary minimum at the T-shaped configuration—remain unaltered.

Almost simultaneously and independently Naumkin (1998) carried out a very similar *ab initio* study (CCSD-T) and obtained results in a qualitative agreement with

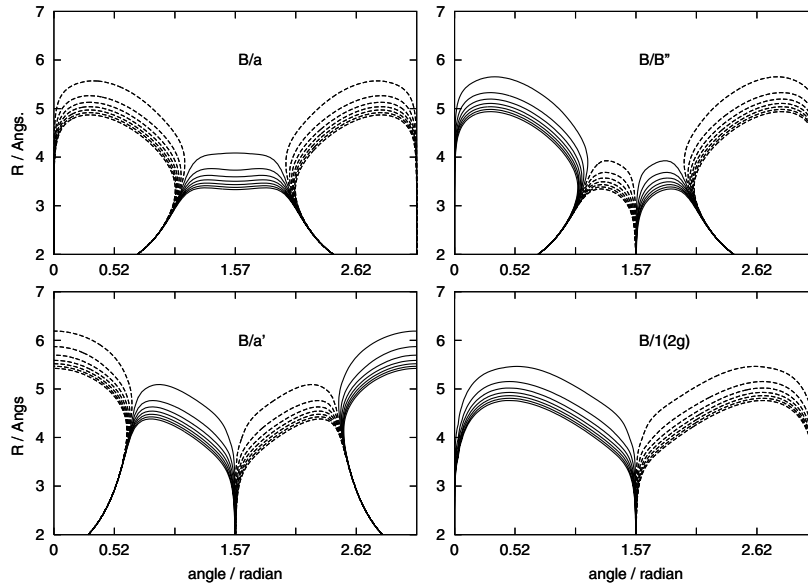

Figure 3. Contour plots of the diabatic coupling matrix elements between the $B(^3\Pi 0_u^+)$ and crossing states of the $Ar\cdots I_2$ complex computed using the DIM PT1 method in Jacobi (R,θ) coordinates. The abscissa is the angle θ between the Jacobi vectors (**R** from Ar to the centre of mass of I_2, **r** linking the I atoms). The ordinate is the distance R between Ar and the centre of mass of I_2. The I_2 distance is taken as the equilibrium value for the B state. Contour lines are drawn from -39 to $39\,cm^{-1}$ with a step of $6\,cm^{-1}$, broken curves correspond to negative values. (Reprinted from Lepetit *et al.* (2002)).

those of Kuntz *et al.* (1998) with a difference of a few tens of wavenumbers due to a smaller basis set (see table 1, entry 11). For the same reason, the calculated binding energies of the $^2\Sigma^+$ and $^2\Pi$ states of the $Ar\cdots I$ fragment underestimate the measured ones (Zhao *et al.* 1994) by 100 and $50\,cm^{-1}$ respectively. Using equation (3) and introducing various corrections to the *ab initio* potentials, Naumkin and McCourt (1998c) constructed a family of improved PESs, one of them giving the dissociation energies $D_0(T,X) = 233\,cm^{-1}$ and $D_0(L,X) = 237\,cm^{-1}$. These results were considered as an argument in favour of Klemperer's energetics of the $Ar\cdots I_2(X)$ complex.

However, later Naumkin (2001) reported an improved *ab initio* study. It used the same CCSD-T methodology with an extended basis set, and incorporated relativistic effective core potential (RECP) for the inner shells of the iodine atoms. As a result, significantly deeper minima were obtained (table 1, entry 12), but the Ar–I interaction remained underestimated by *ca.* $35\,cm^{-1}$. With the help of the Naumkin–Knowles model (equation (3)), the 'best *ab initio* estimations' for $D_0(T,X)$ and $D_0(L,X)$ were obtained as 242 ± 11 and $250 \pm 8\,cm^{-1}$ respectively.

The most recent and accurate calculations on the $Ar\cdots I_2(X)$ PES have been reported by Prosmiti *et al.* (2002b). Although they used practically the same method as Naumkin, a remarkable improvement was achieved by augmenting the AO basis set by bond functions which provide an efficient way of saturating the basis set for a correct treatment of dispersion interaction (Chałasiński and Szczęśniak 1994). The resulting binding energies of both isomers are larger (table 1, entry 13). Calculation of the zero-point energy yielded $D_0(T,X) = 212\,cm^{-1}$ and $D_0(L,X) = 237\,cm^{-1}$.

To summarize, *ab initio* calculations tend to converge the binding energy of the T-shaped isomer to the value conforming with Levy's data. They always predict the linear isomer to be lower in energy, in agreement with the hypothesis of Burke and Klemperer (1993b), but the dissociation energy seems to converge to a larger value than the one obtained by Stevens Miller *et al.* (1999) and to a smaller energy difference with the perpendicular isomer than deduced from intensity ratios in the experiment of Burke and Klemperer.

If the ultimate goal of electronic structure theory is to provide accurate electronic characteristics for the quantitative determination of spectroscopic and dynamical observables, theoretical investigations of $Ar\cdots I_2$ are far from being finished. *Ab initio* and DIM methodologies do not completely agree with each other and with directly determined experimental energies. The dissociation energy of the linear isomer is still uncertain. There is only one experimental result (Stevens Miller *et al.* 1999), which agrees fairly well with one *ab initio* result (Kunz *et al.* 1998) and DIM calculations (Buchachenko *et al.* 2000b), but not with more recent and better converged *ab initio* results (Naumkin 2001, Prosmiti *et al.* 2002b). The dissociation energy of the perpendicular isomer seems to be better established since there are two independent but identical experimental estimates (Blazy *et al.* 1980, Burroughs and Heaven, 2001), supported by recent DIM (Buchachenko *et al.* 2000b) and *ab initio* (Naumkin 2001, Prosmiti *et al.* 2002b) results. The contradicting experimental estimate (Stevens Miller *et al.* 1999) is an indirect one, subject to questions and uncertainties.

4. The one-atom cage effect

Saenger *et al.* (1981) showed evidence for recombination of I_2 excited above the B state dissociation limit when I_2 was complexed with one or more atoms or molecules, whereas uncomplexed I_2 exhibits 100% dissociation (Burde *et al.* 1974). Valentini and Cross (1982) reported the observation of the 'one-atom cage effect' by recording the dispersed fluorescence of recombined $I_2(B)$ produced on excitation of the $Ar\cdots I_2$ complex at 488 nm, 448 cm^{-1} above the B state dissociation limit of I_2. Their results showed that the cage effect produces I_2 in vibrational levels $(23 \leq v' \leq 49)$ that lie from 800 cm^{-1} to more than 2300 cm^{-1} below the initially excited I_2 energy. Such a large energy transfer, much larger than the one observed in vibrational predissociation of $Ar\cdots I_2$ (Johnson *et al.* 1981), was interpreted as a purely kinematic (ballistic) mechanism, namely impulsive transfer from I_2 to Ar which dissociates the complex. A three-dimensional quasi-classical study by Noorbatcha *et al.* (1984), using an empirical pairwise potential with parameters taken from Beswick and Jortner (1978b), indicated that efficient impulsive energy transfer could occur from near-collinear geometries, but the amount of energy transfer was not as large as that measured by Valentini and Cross (1982). An 'anchoring' effect due to the attraction exerted by the argon atom on the departing I atoms from near-T-shape initial geometries could result in long-lived, complex trajectories also leading to stabilization of I_2, but it is a much slower and less efficient energy transfer process. Subsequent, extensive dispersed fluorescence experiments conducted by Philippoz *et al.* (1986, 1987, 1990) on $Rg\cdots I_2$ complexes gave a more complete picture of the one-atom cage effect. They reported product vibrational state distributions obtained at several photodissociation wavelengths (496.5, 488 and 476.5 nm, corresponding to 98, 448 and 943 cm^{-1} respectively above the dissociation

limit) for $Ne\cdots I_2$, $Ar\cdots I_2$, $Kr\cdots I_2$ and $Xe\cdots I_2$. The most probable recoil energy increased with increasing excitation energy and with increasing mass. For $Ar\cdots I_2$, it was around 815, 965 and 1165 cm^{-1} for $\lambda = 496.5$, 488 and 476.5 nm excitation respectively, which was significantly larger than the prediction by Noorbatcha *et al.*

At the time at which these results were obtained, there was no definitive structural information available for the $Ar\cdots I_2$ complex; see preceding section. However, in analogy with $He\cdots I_2$, the common belief was that the $Ar\cdots I_2(X)$ complex had a T-shaped structure. For this structure, a purely kinematic energy transfer cannot be very efficient, which made the one-atom cage effect stand as somewhat of an enigma.

An alternative mechanism for the cage effect was then proposed by Beswick *et al.* (1987), involving two electronic states. In this mechanism, initial continuum excitation is not to the $B(^3\Pi 0_u^+)$ state but to the repulsive $B''\,1_u$ state (figure 1), which contributes significantly to the photon absorption cross-section in the $\lambda = 500$–450 nm wavelength region (Tellinghuisen 1982) (the strength of the $B''\,1_u \leftarrow X(^1\Sigma 0_g^+)$ absorption is about 0.6 that of the $B(^3\Pi 0_u^+) \leftarrow X(^1\Sigma 0_g^+)$ one at 488 nm). The B'' and B states are weakly coupled by magnetic and hyperfine interactions in the free I_2 molecule (Broyer *et al.* 1975, 1976). The presence of a solvent atom or molecule can induce a stronger coupling between these two states; see section 3.5. The proposed mechanism, usually called the 'non-adiabatic cage effect', was then

$$Ar\cdots I_2 \xrightarrow{h\nu} Ar\cdots I_2(B'', E) \xrightarrow{C} Ar + I_2(B, v). \tag{5}$$

If it is assumed that the electronic non-adiabatic coupling C is a slowly varying function of the I_2 internuclear coordinate, the rates for I_2 recombination to the final vibrational levels v of the B state are proportional to the Franck–Condon factors:

$$k_{(B'',E)\rightarrow(B,v')} \propto |\langle \chi_E^{B'} \mid \chi_v^{B} \rangle|^2, \tag{6}$$

where $\chi_E^{B''}$ is the continuum function for the I–I motion in the B'' dissociative state at energy $E = E_0 + h\nu$ and χ_v^B a final vibrational wavefunction in the B state. This model gave final distributions of $I_2(B, v)$ states (Beswick *et al.* 1987, Roncero *et al.* 1994a) very similar to the experimental results of Philippoz *et al.* (1987).

In order to distinguish between the purely kinematic and the non-adiabatic models for the cage effect, Burke and Klemperer (1993b) studied the absorption and fluorescence of $Ar\cdots I_2$ in the bound region of the B state. In that region the $B(^3\Pi 0_u^+) \leftarrow X(^1\Sigma 0_g^+)$ transition intensity is localized in discrete bands, while the $B''\,1_u \leftarrow X(^1\Sigma 0_g^+)$ transition remains a continuum. If the non-adiabatic model were true, exciting between the lines of the $B \leftarrow X$ transition (hence exciting the B'' continuum) would lead to fluorescence from B state I_2, whereas a purely kinematic mechanism would yield dissociation and no fluorescence. The experimental results showed the existence of fluorescence from continuum excitation in the region $v'_B \geq 14$, with a wavelength dependence of the relative intensity that was adequately modelled by the mechanism proposed by Beswick *et al.* (1987), but the measured absolute intensity of the fluorescence was much too large to be due to the sole excitation of the $B''\,1_u$ state. The total continuum intensity integrated over the range of the $I_2(B, v'_B = 26) \leftarrow (X, v'' = 0)$ vibronic band was determined to be 2.1 ± 0.4 times the integrated intensity of the corresponding discrete band of $Ar\cdots I_2$.

However, at this excitation wavelength, the transition intensity to the B″ state is only 0.13 of that to the B state (Tellinghuisen 1982).

Burke and Klemperer proposed that this continuum could be due to the existence of a linear isomer. Brown *et al.* (1985) had reported comparable minima for linear and T-shaped geometries in a calculated potential energy surface for $He \cdots I_2$, but there was no *ab initio* study for $Ar \cdots I_2$ at the time. In contrast to the T-shaped isomer, there could be a large difference in the equilibrium bond length and binding energy of the B state relative to the X state. It was argued that the zero occupancy of the σ^* orbital in the X state may result in a fairly short equilibrium bond length for the linear isomer. On excitation to the B state, a π^* electron is transferred to the σ^* orbital, thus increasing this bond length and lowering the binding energy. This can result in a continuum absorption spectrum for this isomer if the difference in bond lengths is large enough. The linear isomer could then account for the one-atom cage effect observed above the B state dissociation limit by a purely kinematic effect.

A three-dimensional quasi-classical trajectory study by Miranda *et al.* (1994) concluded that the one-atom cage effect could not be due to a linear isomer, using Gray's pairwise interaction potential (Gray 1992); see section 3. Caging was indeed observed, and energy transfer was more important for the linear than for the T-shaped structure, but it was still too low compared with experiments. However, the X state configuration of the linear isomer was only guessed, in the absence of any information. In particular, the Ar–I bond length was taken to be the same as the Ar–I distance in the perpendicular configuration, which was revealed to be wrong in later DIM and *ab initio* studies. In a classical simulation of the $I_2 \cdots Rg_n$ cage effect using empirical potentials (see end of section 3.3), Schröder and Gabriel (1996) concluded that, in order to explain the cage effect, the van der Waals binding energy had to be increased, or more than one rare gas atom had to be bound to I_2 or the configuration of the one-atom complex had to be collinear with a larger I_2–Rg equilibrium distance in the B state compared with the X state.

In a wavepacket calculation restricted to the collinear configuration, Fang and Martens (1996) showed that, by using a model interaction PES deduced from the known $I(^2P_{3/2})$–Ar and $I^*(^2P_{1/2})$–Ar interactions (see section 3.4), good agreement with experiment was obtained. However, it was not clear whether this result would still be valid using the experimentally validated Ar–I_2(B) potential and on going out of the purely collinear configuration (which has strictly speaking a probability of zero because of the solid angle volume element). In a three-dimensional wavepacket study using the *ab initio* PES of Kunz *et al.* (1998) for the X state and the IDIM PT1 PES for the B state, Zamith *et al.* (1999) confirmed the possibility of a purely kinematic origin of the one-atom cage effect from the linear isomer of $Ar \cdots I_2$ and showed that the vibrational distributions depended strongly on the ground- and excited-state equilibrium geometries. A very good agreement with experimental final vibrational distributions was obtained by increasing the equilibrium distance in the I–Ar interaction potentials in IDIM PT1 PES by 2% (figure 4).

Additional experimental indications that the kinematic mechanism of direct, impulsive energy transfer in the collinear isomer is responsible for the one-atom cage effect have been obtained. The existence of two geometrically distinct forms has been demonstrated in the photoionization study of Cockett *et al.* (1996). Burroughs *et al.* (1999) have reported the results of fluorescence-depletion, i.e. 'hole-burning', experiments which demonstrate that fluorescence from free I_2 produced by excitation above the B state dissociation limit is not depleted by excitation to the

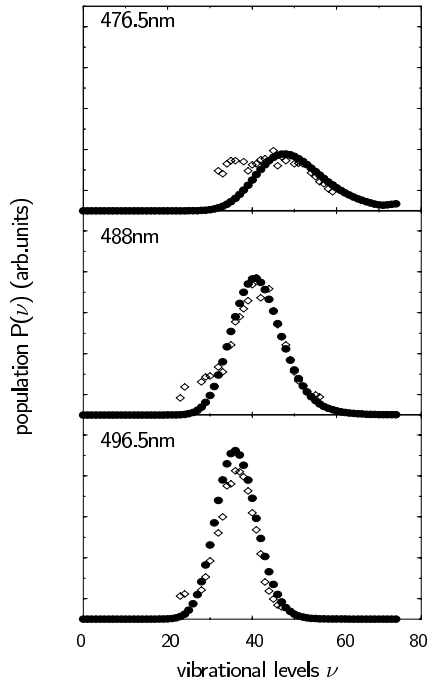

Figure 4. Final vibrational distributions of $I_2(B)$ after excitation of the $Ar\cdots I_2$ van der Waals complex with wavelengths of 476.5, 488, and 496.5 nm: ●, results from the three-dimensional wavepacket calculation (Zamith *et al.* 1999); ◇, experimental results from Philippoz *et al.* (1987). (Reprinted from Zamith *et al.* (1999).)

T-shaped $B \leftarrow X$ band of $Ar\cdots I_2$. Fluorescence depletion was indeed observed by excitation to the adjacent continuum which had been assigned to the linear isomer by Burke and Klemperer (1993b). This shows that, even though direct absorption to the $B''\,1_u$ state exists, non-adiabatic coupling to the B state due to the presence of the argon atom is not strong enough to produce any appreciable amount of caging from the perpendicular isomer. The one-atom cage effect is thus due to the collision of the dissociating I atom with the argon atom near the linear configuration. The same effect was surmised by Wan *et al.* (1997) to explain their experimental results on caging of I_2 by collisions with rare gas atoms at room temperature. It was confirmed in a wavepacket simulation by Meier *et al.* (1998), who obtained very good agreement with the recurrences observed in the pump–probe signal. They observed that effective collisional caging can only occur if the collision leads to a large momentum transfer from the iodine to the Ar atom, which is the case if the collision occurs at small angles, i.e. close to the collinear case, and at small I–I distances, where (because of the well of the B state potential) the relative motion of the dissociating I atoms is fast. This is why it is important for caging in the van der Waals cluster that the intermolecular bond length in the X state be shorter than in the B state: vertical excitation brings $Ar\cdots I_2$ close to the hard sphere collision distance in the B state, so that one of the departing I atoms hits the argon with a high velocity, therefore transferring a large amount of momentum.

Caging of I_2 was also observed in large rare gas clusters (Liu *et al.* 1993) and matrices (Beeken *et al.* 1983, Macler and Heaven 1991, Zadoyan *et al.* 1994a,b, Benderskii *et al.* 1997). Many of the matrix studies were done in the bound state

region of the B state, where the process is more complex. It first implies electronic predissociation of the B state, followed by caging, or initial excitation to the dissociative B'' or the repulsive region of the weakly bound $A\,1_u$ state. Fluorescence from B state recombined I_2 was indeed observed. In addition, infrared emission was also detected from the $A\,1_u$ and $A'\,2_u$ states which are weakly bound states going to the $(I^2P_{3/2}) + I(^2P_{3/2})$ dissociation limit. Batista and Cocker (1997) conducted a non-adiabatic molecular dynamics simulation of a time-resolved pump–probe experiment of A and B state I_2 in a rare gas matrix, similar to the experiments by Apkarian and coworkers (Zadoyan *et al.* 1996). In the region of the B state excitation, they do not consider the possible excitation to the A or $B''\,1_u$ states which also contribute to the absorption cross-section. However, the dynamics following excitation to the B state is rich and complex. The excited molecules can either remain in the B state or predissociate to one of the three $B''\,1_u$, $1\,2_g$, or a 1_g states during their early time dynamics. The predissociated molecules recombine after hitting the cage atoms into the $A\,1_u$, $A'\,2_u$, and X states. It can be noted that I_2 occupies initially a double substitution site in an undistorted f.c.c. argon crystal, which puts it in a collinear configuration with some of its nearest neighbours. This is clearly a different situation from exciting I_2 above its B state dissociation limit where dissociation is direct. However, it does show that non-adiabatic effects can be quite important in the condensed phase. One important difference with the one-atom cage effect is that the argon atoms do not evaporate, so that, when the I–I distance is very long and the I atoms collide with the argon atoms of the cage, they feel a strong I–Ar interaction which couples the I_2 states.

Solvent-induced dissociation and caging dynamics of $I_2(B)$ was also studied by a time-resolved pump–probe experiment in supercritical rare gas solvents (Lienau and Zewail 1996) and the role of the A and A' states was again put in evidence. It would be interesting to look for the possibility of observing these states in the one-atom cage effect.

5. VP, IVR and spectra

5.1. *Experimental data for the T-shaped isomer VP dynamics*

When the $Rg \cdots I_2$ van der Waals molecules are excited in the bound spectral region of $I_2(B)$, the fluorescence excitation spectra show broadened features associated with $Rg \cdots I_2(B, v')$ quasi-bound levels which decay into a dissociative continuum by predissociation.

The first complex investigated in this family was $He \cdots I_2$ (Smalley *et al.* 1976, Johnson *et al.* 1978, Sharfin *et al.* 1979) reviewed in Levy (1981). Levy and coworkers determined the broadening of the lines as a function of v', the vibrational excitation of $I_2(B)$ within the complex, by detecting the fluorescence of the $I_2(B, v < v')$ products. The width of the peaks showed a monotonic increase as a function of v', the $v = v' - 1$ vibrational level of I_2 being the dominant final state, by more than 90%. Soon after the first measurements, Beswick and Jortner (1977, 1978a,b, 1981), Ewing (1979), and others (Beswick *et al.* 1979, Beswick and Jortner 1980, Delgado-Barrio *et al.* 1983), interpreted these results in terms of the energy or momentum gap law: the coupling between the $He \cdots I_2(B, v')$ quasi-bound state and the $He + I_2(B, v' - 1)$ dissociative continuum grows larger as the final kinetic energy between the fragments decreases.

However, at higher excitation energies, when the $\Delta v = -1$ channel closes, the monotonic increase of the measured linewidths with v' suddenly stops and thereafter behaves erratically with v'. This behaviour has been observed for complexes such as $He\cdots I_2$, $Ne\cdots I_2$, $He\cdots Br_2$ (van der Burgt and Heaven 1984, Jahn *et al.* 1994, 1996), $Ne\cdots Br_2$ (Cline *et al.* 1987) or $Ar\cdots Cl_2$ (Evard *et al.* 1988a). This is due to the presence of secondary quasi-bound states associated with the closed $v'-1$ channels (Roncero *et al.* 1988, Halberstadt *et al.* 1992a,b, González-Lezana *et al.* 1996). Dissociation now occurs predominantly in a stepwise fashion: $Rg\cdots X_2(n', v') \rightarrow Rg\cdots X_2(n'' > n', v'-1) \rightarrow Rg + X_2(v = v'-2)$. This mechanism corresponds to the IVR process, where vibrational quanta are transferred in a sequential fashion from the stretching mode of the I–I molecule to van der Waals modes (with an excitation defined by a collective quantum number n) until this weak bond breaks. Because the energy difference between the interacting initial 'bright' and intermediate 'dark' quasi-bound states changes as a function of v', the rate of dissociation depends strongly on v' in a very oscillatory way. The erratic dependence of the VP rate as a function of initial excitation is a fingerprint that IVR is in the sparse regime (the different IVR regimes are presented in appendix 2). Sparse IVR has a second observable fingerprint on rotational distributions, as shown in $Ar\cdots Cl_2$ (Evard *et al.* 1988a) and $He\cdots Br_2$ (Rohrbacher *et al.* 1999a). Since the 'dark' state acts as a doorway for dissociation, the final rotational distribution of the halogen fragments depends strongly on the nature of the 'dark' state, especially on its bending character. As a result, complicated oscillatory rotational distributions which depend strongly on the initial excitation are obtained in this regime. In addition, because of the I_2 anharmonicity, the relative energies of bright and dark states change with v' and so does the bending character of the doorway state. Thus, rotational distributions are strongly dependent on the initial excitation.

The dynamics of $Ar\cdots I_2$ complexes presents special features as compared with the lighter complexes of the same family. One is the balanced competition between EP and VP, which is analysed in section 6. Another is related to the final vibrational state distribution of the $I_2(B, v)$ products after excitation of $Ar\cdots I_2(B, v')$, as measured by Levy and coworkers (Johnson *et al.* 1981): they found that the first open channel is $v'-3$. This results from the value of the binding energy of the $Ar\cdots I_2(B)$ complex, which is believed to be larger than two vibrational quanta of the uncomplexed $I_2(B)$ molecule in the energy region of interest (see section 3). The stepwise mechanism now involves two sets of intermediate 'dark' states $Ar\cdots I_2(n'' > n', v'-1)$ and $Ar\cdots I_2(n''' > n'', v'-2)$. Because of this increase of intermediate level density, one may wonder whether IVR still occurs in the sparse regime or approaches intermediate or even statistical regimes (see appendix 2). This question is still open. On the one hand, real-time picosecond measurements have shown that the kinetics of formation of the I_2 product follows a simple exponential law (Breen *et al.* 1990, Willberg *et al.* 1992). Also, the decay rates appear not to be significantly modified by initial van der Waals excitation (Burke and Klemperer 1993a). These facts advocate a dense regime IVR. Assuming such a regime, VP rate is expected to increase monotonically with v', and EP would be responsible for the oscillations in the fluorescence intensity, as will be discussed later in section 6. However, experimental product rotational distributions (Burroughs and Heaven 2001) show structures which are reminiscent of sparse regime IVR, an idea which is also supported by all recent quantum calculations on this system. Addressing the

problem of the IVR regime in VP dynamics should also help in understanding the origin of the oscillations in the fluorescence intensity.

5.2. *Theoretical interpretations for the T-shaped isomer VP dynamics*

As in the $He\cdots I_2$ case, the first theoretical modelling of $Ar\cdots I_2$ assumed a direct mechanism in the collinear geometry within a distorted wave approximation (Beswick and Jortner 1980) and found a monotonic increase of the VP rate with increasing v'. In addition, the VP rates were in rather good agreement with those obtained in real-time experiments (Breen *et al.* 1990, Willberg *et al.* 1992). This apparent good agreement between theory and experiment fails when it is considered, as noted by Burke and Klemperer (1993a), that the transitions studied correspond to a T-shaped complex.

The first quantum three-dimensional calculations on $Ar\cdots I_2$ were performed by Gray (1992) using a time-dependent wavepacket method and accurate empirical pairwise PES. He found that the population decrease of the initial state does not follow an exponential law, as is the case for the direct mechanism, but presents oscillations attributed to the presence of several resonances with energies and widths obtained by de Prony's method. Thus, using the dominant resonance width, Gray found that the ratio of linewidths $\Gamma_{v'=21}/\Gamma_{v'=18}$ was consistent with the experimental one obtained from the total rates measured by Zewail and coworkers (Breen *et al.* 1990, Willberg *et al.* 1992) and the VP efficiencies obtained by Goldstein *et al.* (1986).

The influence of IVR on the VP dynamics of $Ar\cdots I_2$ was later analysed (Gray and Roncero 1995, Roncero and Gray 1996) using time-dependent as well as time-independent calculations on the same PES. These essentially exact calculations (from the dynamical point of view) were nicely reproduced by approximate analytical models based on standard radiationless transition treatments (Roncero and Gray 1996), extending work already performed on $Ar\cdots Cl_2$ (Halberstadt *et al.* 1992a,b).

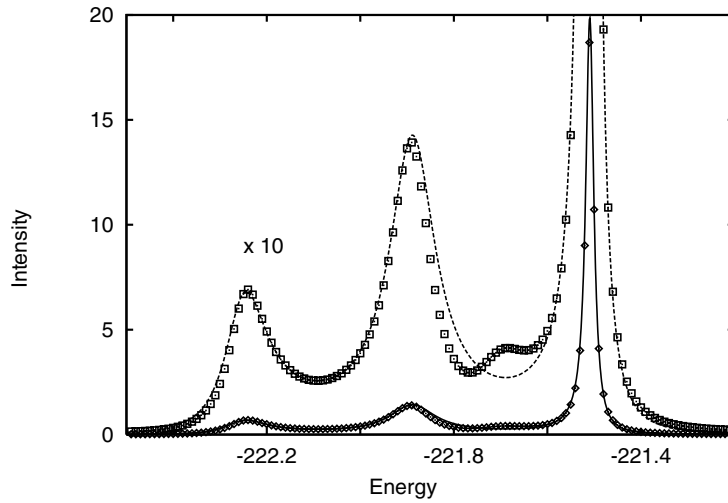

Figure 5. Spectrum associated with the initial state $Ar\cdots I_2(B, v'=21, n'=0)$ with zero total angular momentum: the points correspond to numerical time-independent calculations, the full and broken curves to an analytical radiationless model based on three zero-order bound states. Magnification by a factor of 10 gives a better view of the details. (Reprinted from Roncero and Gray (1996).)

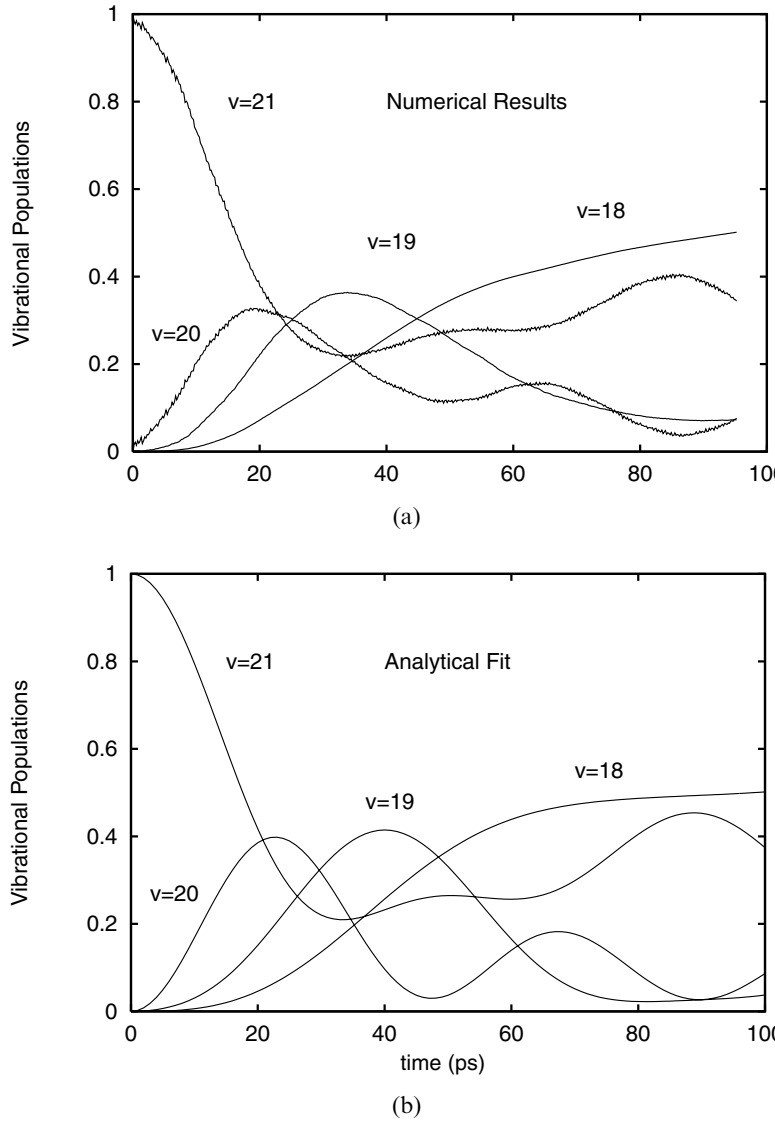

Figure 6. Vibrational population of the $I_2(B)$ fragment as a function of time for the initial state $Ar\cdots I_2(B, v' = 21, n' = 0)$, zero total angular momentum: (*a*) numerical time-dependent results; (*b*) analytical model with adjusted parameters. (Reprinted from Roncero and Gray (1996).)

It was possible to characterize in detail the number and the nature of the zero-order bound states involved. As an example, the absorption spectrum and vibrational population versus time are shown in figures 5 and 6, respectively for the VP of $Ar\cdots I_2(B, v' = 21)$. The analytical model requires only a few bound states, three in this particular case, belonging to the v' (bright state), $v' - 1$ and $v' - 2$ (dark states) manifolds. As already noted, three vibrational quanta are required to fragment the $Ar\cdots I_2$ complex, and it can be clearly considered as a sequential mechanism as was the case in $Ar\cdots Cl_2$. The population, initially in the v' channel, is transfered to $v' - 1$. Once the population in the $v' - 1$ channel becomes significant, population

starts building up in channel $v'-2$, and dissociation starts in channel $v'-3$ once there is enough population in $v'-2$. Because of this sequential mechanism, the dissociation probability shows a clear non-exponential behaviour (Roncero *et al.* 1993, 1997). The exact picture is a bit more complicated, however. At each vibrational step, the population bifurcates to go not only to the $v-1$ manifold but also to the $v+1$ one. In addition, there are contributions from other energy pathways involving steps with the transfer of more than one quantum. As a conclusion, it was found that the VP of $Ar\cdots I_2$ is mediated by IVR, involving only a few zero-order bound states (sparse limit). Because the coupling between those few bound states depends on their mutual separation, it was found (Gray and Roncero 1995, Roncero and Gray 1996) that the VP rate presents oscillations as a function of v'.

How can these oscillations be reconciled with the experimental assumption of a monotonic dependence of the VP rate, made by Burke and Klemperer (1993a) in order to interpret the relative efficiencies of the VP and EP processes (see section 6 for details)? This monotonic increase is the fingerprint of IVR in the statistical limit, where the 'bright' state always 'faces' a second 'dark' state owing to their relatively high density. The possibilities for explaining the discrepancies in the dependence of the VP rate on v' are the following:

(1) The potential is inadequate to describe VP. However, several parametrizations were used (Roncero and Gray 1996) and the sparse limit IVR was obtained in all calculations.
(2) The widths of the dark states may be increased by coupling to the continuum through EP, thus changing the IVR regime (see section 6).
(3) For such heavy systems, the total angular momentum can be quite large and the density of states is expected to increase. Also, rotational averaging corresponding to the experimental conditions may smooth out VP rate oscillations.

Let us consider in more detail the effect of the total angular momentum on the VP dynamics. Some early time-independent calculations on $Ar\cdots Cl_2$ showed an extreme sensitivity not only to the value of J but also to its projection on a body-fixed frame axis (Roncero *et al.* 1993). The same situation occurred for $Ar\cdots I_2$ for low angular momentum. Time-dependent and time-independent calculations showed the sensitivity due to the change in the relative energies of the 'dark' and 'bright' states as a function of J (indeed, dark states have smaller rotational constants than bright ones, being more excited in the van der Waals mode (Roncero *et al.* 1993)).

Following this line, time-dependent calculations for high J values were performed for $Ar\cdots I_2$, by Goldfield and Gray (1997a,b), and for $Ar\cdots Cl_2$ by Roncero *et al.* (1997). When J values were varied up to 15 or 20, the IVR regime remained in the sparse–intermediate regime if the initial rotational sublevel K (where K denotes the $2J+1$ sublevels by increasing energy order) is small and unchanged. However, when both J and K are modified, the effect is larger (Roncero *et al.* 1997). A good example is provided by $Ar\cdots Cl_2(B, v'=18)$, where three vibrational quanta are required to fragment the complex as in $Ar\cdots I_2$ (see figure 7). In this case for $J=0$ and for ($J=15$, $K=1$) the autocorrelation functions show clear recurrences attributed to sparse–intermediate regimes, while for ($J=15$, $K=2J$) the recurrences tend to disappear, clearly showing a tendency towards the statistical limit. This was shown to reflect the character of the initial bright state due to Coriolis coupling on

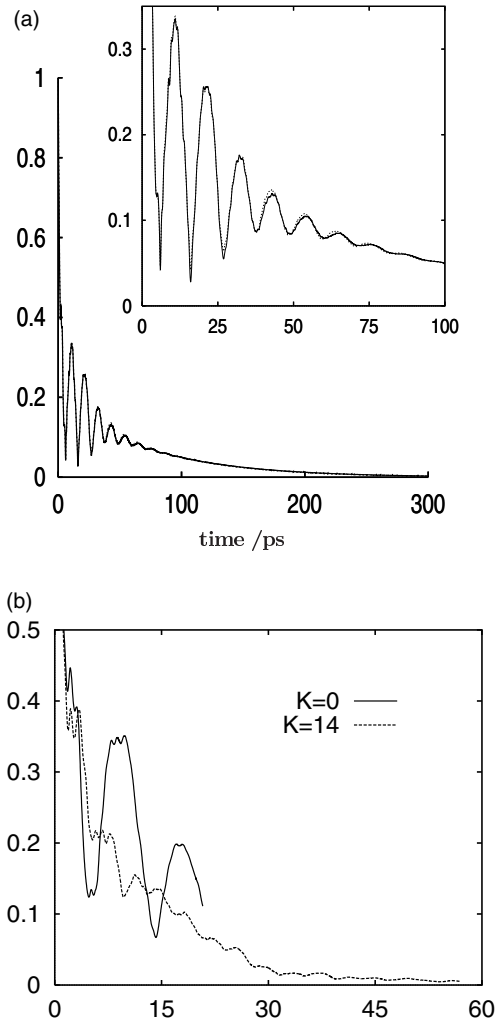

Figure 7. Norm of the autocorrelation function for $Ar\cdots Cl_2(B, v' = 18, n' = 0)$. (*a*) J = 0. The insert gives the details at short times. The full curve is the result of a wavepacket calculation, the broken curve corresponds to an analytical fit of the spectrum in terms of independent resonances. (*b*) J = 15, $K = 0$ (full curve) and $K = 14$ (broken curve). (Reprinted from Roncero *et al.* (1997).)

the bound states rather than the effect of the Coriolis coupling on the dynamics, which is rather weak. The bright state $K = 0$ is mainly of $\Omega = 0$ character, where Ω stands for the projection of the total angular momentum on the axis which connects Ar to the centre of mass of the dihalogen. Bright states corresponding to large K have components on a larger range of Ω values. As a result, more dark states are involved in the dissociation dynamics of a large K bright state than of a low K one. However, another calculation on $Ar\cdots I_2$ (Goldfield and Gray 1997a,b) was performed for $J = 10$, and a sparse limit IVR was obtained. Therefore, more complete calculations, including higher angular momenta, proper average over the initial thermal rotational distribution and taking into account EP channels, would be most useful to elucidate the role of the total angular momentum in $Ar\cdots I_2$.

Another way to modify the IVR regime is to increase the initial vibrational excitation of the diatomic subunit. One may expect that the increase of dark state density induced by the anharmonicity will change the IVR regime from a sparse to a dense one. This has been observed in $Ar\cdots Cl_2$ (Roncero *et al.* 1997) and $Ne\cdots Br_2$ (Roncero *et al.* 2001a): the IVR bands associated with increasing v' values become more and more congested. However, close to the dissociation limit, some narrow peaks suddenly appear again, associated with resonances where the rare gas atom is inserted between the two halogen atoms (Roncero *et al.* 2001a, Prosmiti *et al.* 2002c). The halogen diatomic is so stretched that VP becomes inefficient, thus introducing some sparse character in the spectra. It would be interesting to perform a similar study on $Ar\cdots I_2$.

5.3. *Comparative spectra of the perpendicular and linear isomers and discussion of their binding energies*

The goal of this section is to give a comparison of the energy levels and absorption spectroscopy calculated for the two different isomers of $Ar\cdots I_2$ and to discuss their energetics. The discussion of the spectra will be based on the DIM PT1 surfaces, for both the X (Buchachenko *et al.* 2000b) and the B (equation (4)) states. Note that these surfaces gave very reasonable agreement with the product state distributions from $Ar + I_2(B)$ vibrationally-inelastic collisions measured in the bulk and in molecular beams (Buchachenko and Stepanov 1998b). The topology of these PESs is illustrated in figure 2, while the properties of their minima are presented in table 1.

The contour plots of the calculated vibrational wavefunctions for zero total angular momentum (Roncero *et al.* 2001b) are presented in figure 8 for the lowest van der Waals levels of the X state (r fixed at its equilibrium value) and of the $(B, v = 21)$ states (Buchachenko *et al.* 2000b, Roncero *et al.* 2001b). The ground $n_X = 0$ van der Waals level of the X state has a dissociation energy of $208.9\,cm^{-1}$ and corresponds to the T-shaped isomer, as well as the next four levels. The ground state of the linear isomer appears as a degenerate doublet, $n_X = 5$ and $n_X = 6$, corresponding to opposite I–I permutation symmetries. Their energy determines the dissociation energy of the linear isomer. The dissociation energies of both isomers are listed in table 2 together with other theoretical and experimental estimations.

The wavefunctions of the $(B, v = 21)$ levels n_B are plotted in the bottom panel of figure 8. The lowest-level wavefunctions can be assigned to stretching and bending modes from their nodal pattern, but they become more and more complex and delocalized as energy increases. The linear configuration is a saddle point for the B state PES, so only highly excited bending levels have appreciable amplitude density in this region.

The distinct nature of the T-shaped and linear isomers of $Ar\cdots I_2$ for the DIM PT1 potentials has a direct consequence on $B \leftarrow X$ absorption spectra. Since both the X and the B potentials are similar in the region of the T-shaped well, the Franck–Condon principle implies that the transition probability from the $n_X = 0$ level will be largest for $n_B = 0$ and will rapidly decrease for higher n_B. In contrast, the ground level of the linear isomer has significant overlap integrals only with high n_B levels whose wavefunctions are markedly delocalized near the linear configuration.

These trends indeed define the structure of absorption spectra calculated by means of numerically exact line shape and wavepacket methods. Figure 9 shows the

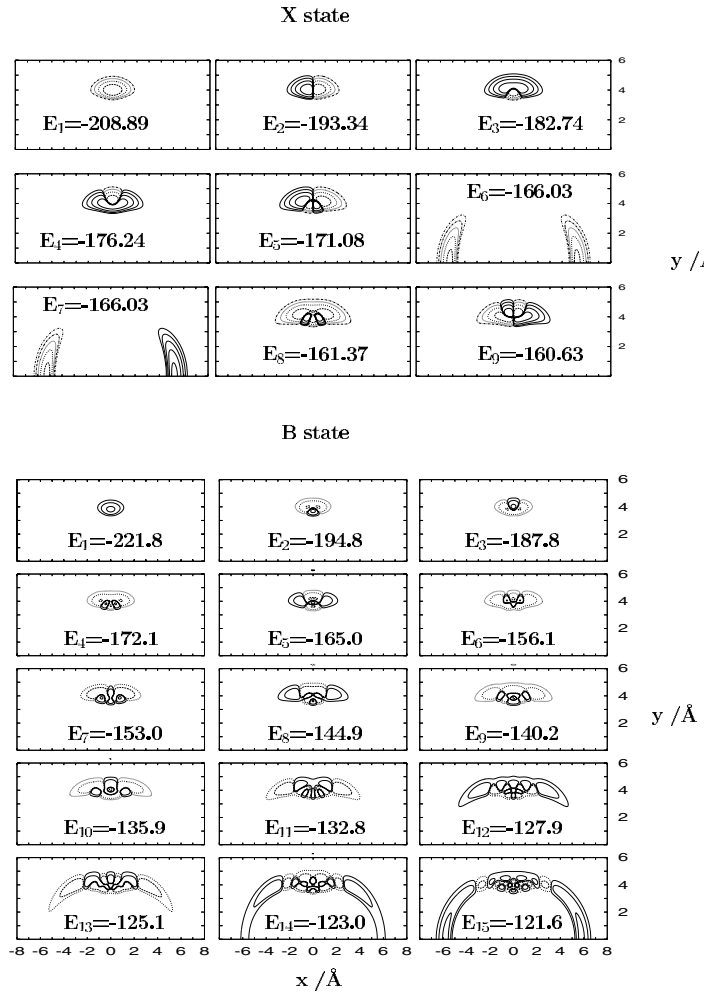

Figure 8. Top panels: contour plots of the amplitude densities of the lowest bound levels of $Ar\cdots I_2(X, J = 0)$ computed at equilibrium I_2 distance for the DIM PT1 potential. Broken curves correspond to negative amplitudes. Abcissae and ordinates are defined as in figure 2. Zero energy corresponds to the $Ar + I_2(X, v = 0)$ dissociation limit. Bottom panels: contour plots of the amplitude densities of $Ar\cdots I_2(B, v = 21, J = 0)$ states (even permutation symmetry of the I nuclei). Broken curves correspond to negative amplitudes. Abcissae and ordinates are defined as in figure 2. Zero energy corresponds to the $Ar + I_2(B, v = 21)$ dissociation limit. (Reprinted from Roncero *et al.* (2001b).)

$B \leftarrow (X, v'' = 0)$ absorption spectra for the $0^{++} \leftarrow 1^{--}$ rotational transition obtained with the DIM PT1 X and B PESs for the T-shaped and linear isomers (upper and lower panels respectively) (Roncero *et al.* 2001b). The spectrum of the T-shaped isomer exhibits a sequence of bands assigned to definite vibrational states v' of $I_2(B)$. For each v' there are three main lines, corresponding to transitions to the ground and the two first van der Waals excited levels. This picture is in perfect agreement with all experimental $B \leftarrow X$ absorption spectra (Johnson *et al.* 1981, Burke and Klemperer 1993a, Burroughs and Heaven 2001).

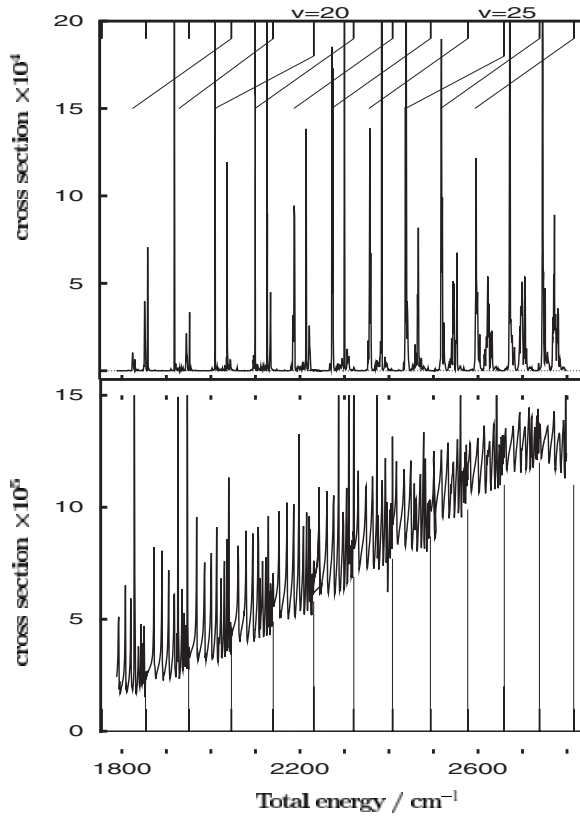

Figure 9. The $(\mathrm{B}, v, J = 0^{++}) \leftarrow (\mathrm{X}, v = 0, J = 1^{--})$ $\mathrm{Ar}\cdots\mathrm{I}_2$ absorption spectra calculated for the T-shaped (top panel) and linear (bottom panel) isomers using the DIM PT1 PES. The $\pm$ superscripts refer to the parity (with respect to inversion of the coordinates) and permutation symmetry (with respect to the exchange of the iodine atoms) of the initial or final states. Note the difference in scale for the absorption cross-sections for the T-shaped and linear isomers. (Reprinted from Roncero *et al.* (2001b).)

In contrast, the absorption of the linear isomer is mostly continuous. Its intensity rises with energy, but by steps rather than monotonically. These steps correlate with the successive opening of new (B, v') vibrational manifolds. A broad, quasi-discrete structure is superimposed on this continuous background. This corresponds to the excitation of highly excited intermolecular levels with a wavefunction sufficiently delocalized to be accessible from the X state linear isomer; see figure 8.

The analysis of the spectral intensity distribution can shed some light on the discussion about the dissociation energy of the isomers presented in section 3.2. The main assumption used by Klemperer and coworkers (Burke and Klemperer 1993b) to deduce the proportion of the two isomers from the absorption spectra is to assign the discrete part to the T-shaped configuration and the continuous part to the linear configuration. The intensity ratio of the linear and T-shaped isomer absorptions derived from the calculations with the DIM PT1 PES is shown in figure 10. It is a highly oscillatory function of energy, with minima and maxima corresponding to the quasi-discrete contributions of the T-shaped and linear isomers respectively. Between these huge oscillations, one can estimate the baseline declining more or less regularly

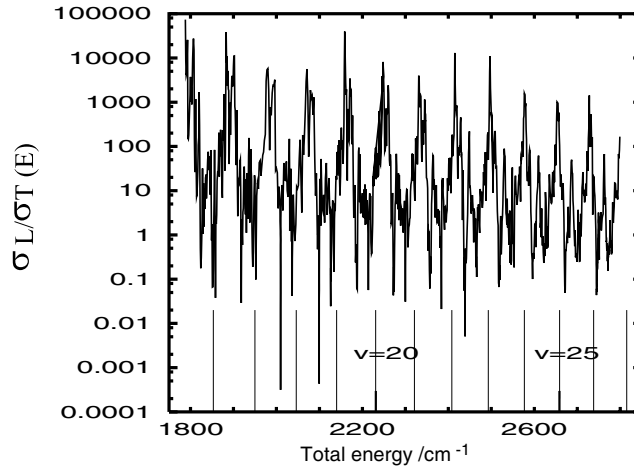

Figure 10. Ratio of absorption cross-sections of the linear and T-shaped isomers for the DIM PT1 PES. (Reprinted from Roncero *et al.* (2001b).)

from 20 to 1. If in addition one takes into account the experimental resolution and the overlapping contributions from many thermally populated rotational levels, the quantitative separation of the two isomers' absorption is clearly a very difficult problem.

A rough estimate of the correction to Burke and Klemperer's value can be made as follows. The experimental continuum intensity integrated over the range of the I_2 $B \leftarrow X$ (26,0) vibronic band is 2.1 ± 0.4 times the integrated intensity of the discrete $B \leftarrow X$ (26,0) band of $Ar \cdots I_2$ (Burke and Klemperer 1993b). This linear to T-shaped intensity ratio can be written as $I_{exp}(L)/I_{exp}(T) \simeq \langle I(L)/I(T)\rangle (P(L)/P(T)$ where $\langle I(L)/I(T)\rangle$ is the average intensity ratio (for equal population) of the linear versus T-shaped isomer, and $P(L)/P(T)$ is the linear to T-shaped population ratio at an experimental temperature of about 15 K. The average intensity ratio $\langle I(L)/I(T)\rangle$ can be estimated from figure 10 as 10, which would give a population ratio deduced from experiment $P(L)/P(T) = 2.1/10 = 0.21$ instead of 3. This may result in a T-shaped isomer which is more bound than the linear one. Although these estimations are rather crude, they give a correction in the right direction to reconcile the experimental measurements of $D_0(L, X)$ by Stevens Miller *et al.* and of $D_0(T, X)$ by Levy and coworkers. Another source of experimental error could be the saturation of the discrete absorption lines (Klemperer 2001) in the experiment by Burke and Klemperer (1993b), which could lead to an overestimation of the continuum absorption and hence of the linear:T-shaped population ratio.

5.4. *Final VP product state distributions for both isomers*

The final vibrational product state distribution of $I_2(B)$ fragments obtained for the linear isomer is very broad (Stevens Miller *et al.* 1999), while that of the T-shaped extends over few vibrational channels, with the first open channel being the most probable one (Johnson *et al.* 1981). Also, the final rotational distributions obtained from the linear isomer are broad with a maximum at relatively low j values (Burroughs and Heaven 2001), while that from the T-shaped isomer is very complicated and presents several oscillations as a function of j (Burroughs and Heaven 2001). This can be understood as an indirect indication of the IVR-mediated

fragmentation mechanism. These features were qualitatively reproduced by recent quantum calculations (Roncero *et al.* 2001b) performed with only the B electronic state, thus neglecting the EP dissociation channel.

These differences between the final distributions of $I_2(B)$ fragments are due to important differences in the dynamics. The absorption spectrum from the T-shaped isomer is formed by relatively narrow bands, showing that the dissociation dynamics is rather slow. For the linear isomer, however, the situation is completely different: the spectrum is very broad and hence the dynamics very fast. This is because vibrational energy transfer is more efficient at collinear geometries. Also, the initial linear bound states overlap not only with quasi-bound states of $Ar\cdots I_2(B, v')$ (essentially those with large probability at the collinear geometry) but also with continuum states, which dissociate instantly.

6. Electronic relaxation and the competition with vibrational relaxation

6.1. *Competition between EP and VP in the $Ar\cdots I_2$ van der Waals complex: experimental evidence*

As was already noted, the first experimental evidence of existence of the $Ar\cdots I_2$ van der Waals complex was obtained by Levy and his team (Kubiak *et al.* 1978, Levy 1981). The complex was produced in a supersonic expansion of I_2 and the fluorescence excitation spectrum was observed, only for vibrational excitation of $I_2(B)$ higher than $v' = 12$. The van der Waals laser-induced fluorescence (LIF) is an

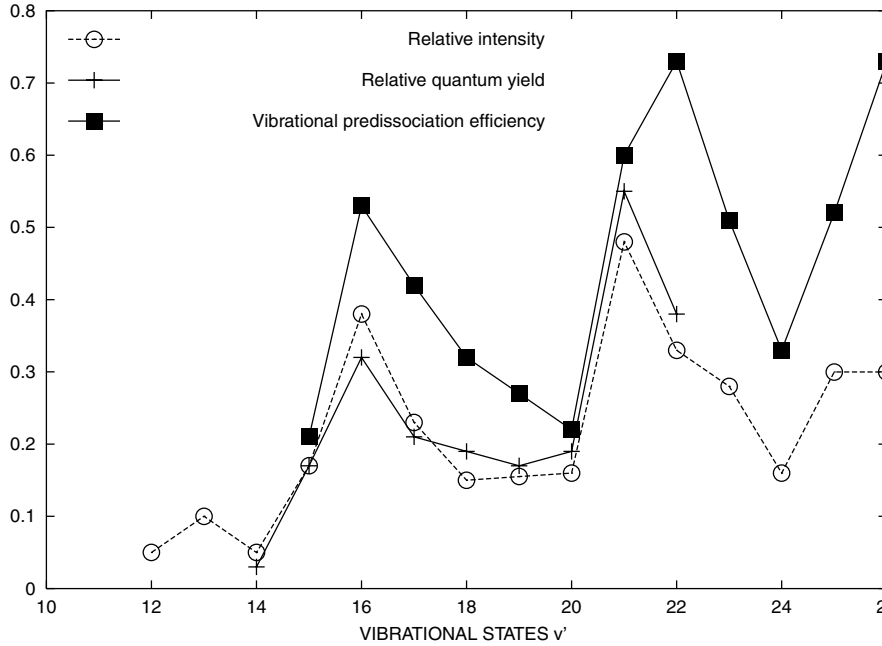

Figure 11. Curve labelled relative intensity: relative intensity of the fluorescence excitation spectrum of $Ar\cdots I_2$ as a function of the vibrational state v' of I_2 that was originally excited. The original data from Levy (1981) have been multiplied by a factor of 10 to match the other results. Curve labelled relative quantum yield: LIF intensity divided by absorbance from Goldstein *et al.* (1986). Curve labelled vibrational predissociation efficiency: relative quantum yield corrected for the Franck–Condon factors for I_2 absorption in v' and I_2 emission in $v' - 3$, from Burke and Klemperer (1993a).

oscillatory function of the $I_2(B)$ vibrational excitation (see figure 11). This behaviour was interpreted as the result of the competition between VP and EP. Since only VP produces a fluorescent product, the LIF intensity depends on the relative efficiency of the VP and EP processes, and the vibrational dependence of the LIF intensity is directly related to the vibrational dependence of the branching ratio. It was speculated that, in analogy with $He \cdots I_2$, the VP rate would be a monotonically increasing function of vibrational excitation. The oscillations in the branching ratio would reflect similar ones in the EP rate, induced by changes in the Franck–Condon factors between bound vibrational states of $I_2(B)$ and vibrational continuum states related to some still unidentified repulsive electronic state.

Later experiments confirmed the initial experimental evidence of Kubiak *et al.* (1978), but contradictory interpretations were proposed. Goldstein *et al.* (1986) measured absorption spectra using intracavity laser spectroscopy (ILS) in conjunction with LIF spectra for the series of $Rg \cdots I_2$ complexes. The ratio of LIF:ILS intensities provides a direct measurement of the relative population of I_2 produced by VP, referenced to the $Rg \cdots I_2$ population. In other words, it provides a measurement of the VP efficiency with respect to EP, provided that corrections for different Franck–Condon factors for emission and absorption are made. For instance, in the case of $He \cdots I_2$ where EP is weak, the LIF:ILS intensity ratio was found to be close to 1: almost all the $He \cdots I_2$ complexes dissociate through VP (Goldstein *et al.* 1986). In the case of $Kr \cdots I_2$ or $Xe \cdots I_2$, only ILS is not negligible. This is an indication that the complex decays predominantly through the EP dark process. Finally, for $Ar \cdots I_2$, the ratio was found to be an oscillatory function of I_2 vibrational excitation for $12 < v' < 26$, with a maximum near 0.5 (see figure 11). This indicates that EP and VP compete with comparable efficiencies. Although these oscillations are similar to those already observed by Kubiak *et al.* (1978), Goldstein *et al.* interpret them as the result of IVR in the VP process, inducing oscillations in the VP rate.

A final experimental confirmation of the results of Kubiak *et al.* and Goldstein *et al.* came with a simultaneous measurement of absorption and fluorescence by Burke and Klemperer (1993a) (see figure 11). The fluorescence:absorption ratio, corrected by different Franck–Condon factors for emission and absorption, yielded a VP efficiency (VPE) which oscillates with the vibrational quantum number similarly to the previous results. In addition, Burke and Klemperer looked at fluorescence intensities corresponding to excitation in the van der Waals modes and found a VPE which oscillates as a function of I_2 stretching similarly to the corresponding VPE for the ground van der Waals mode. They concluded that the oscillations could not be due to accidental degeneracies in the sparse limit IVR process but resulted from Franck–Condon factor oscillations in the EP process. They also conjectured that the $a\,1_g$ state is the one responsible for the EP process. Indeed, they noted that among the states which intersect $B(^3\Pi 0_g^+)$, a 1_g is the only one to be coupled to B for the strictly T-shaped isomer. Moreover, they noted similarities between the oscillations in the electric field quenching rate of the bare $I_2(B)$ molecule (Dalby *et al.* 1984) and the ones in the VPE. They concluded that the same $a\,1_g$ repulsive state must be responsible for both processes.

The experimental results described so far provide information only on relative efficiencies between competing processes, not on absolute rate constants. These could be obtained in principle from homogeneous line widths in fluorescence excitation spectra. Unfortunately, these widths are difficult to measure because of rotational

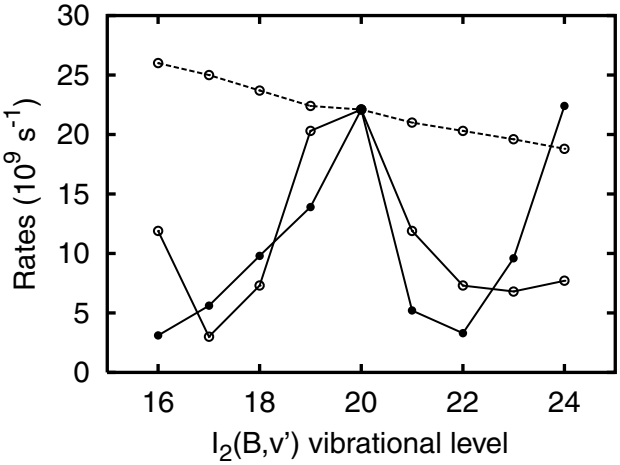

Figure 12. Calculated versus experimental rates for the EP of $Ar\cdots I_2(B, v')$, $v' = 16$–24. The results were scaled such that the EP line width coincides with the experimental one for $v' = 20$. The full dots represent the experimental data of Burke and Klemperer (1993a). The open dots represent the results of a three-dimensional wavepacket calculation for EP by the $a\,1_g$ state. The full and broken curves correspond to an attractive and a repulsive van der Waals interaction in the $a\,1_g$ state respectively. (Reprinted from Roncero *et al.* (1996).)

congestion. Rough estimates could be obtained for instance for $He\cdots I_2$ or $Ne\cdots I_2$ (Kenny *et al.* 1980a), but no published results are available for $Ar\cdots I_2$. However, using picosecond pump–probe techniques, Zewail and his group (Breen *et al.* 1990, Willberg *et al.* 1992) measured the time dependence of the nascent $I_2(v'-3)$ population resulting from VP and deduced total $Ar\cdots I_2(v')$ predissociation rates, including both EP and VP contributions, of 0.014 ps^{-1} for $v' = 18$ and 0.013 ps^{-1} for $v' = 21$. Unfortunately, these measurements were restricted to these two I_2 vibrational excitations.

From these total predissociation rates and branching ratios, Burke and Klemperer (1993a) could obtain individual EP and VP rates for $v' = 18$ and 21. Assuming that the VP rate increases smoothly and semilinearly with vibrational excitation, they could extrapolate EP rates to the whole range of vibrational excitation from $v' = 16$ to 24. Thus, they obtained an EP rate which oscillates with vibrational excitation, as shown in figure 12.

6.2. *Competition between EP and VP in the $Ar\cdots I_2$ Van der Waals complex: theoretical interpretation*

One of the first goals of the theoretical models was to provide an accurate description for the oscillations of EP as a function of vibrational excitation, as obtained from the analysis of Burke and Klemperer (1993a). EP can be well described within the Fermi golden rule approximation as an inital quasi-bound state $Ar\cdots I_2(B)$ decaying into a continuum representing the final dissociative electronic state. The zero-order quasi-bound $Ar\cdots I_2(B)$ state can be represented by:

$$\phi_{v'n}(r, R, \theta) = \phi_{v'}(r)\phi_{nv'}(r, \theta) \tag{7}$$

where r is the I–I distance and R the one from Ar to the I_2 centre of mass, θ the angle between the two corresponding Jacobi vectors, v' the initial vibrational exitation of I_2 and n a collective quantum number for the van der Waals modes. The final state of the EP process is some continuum state $\phi_{Ef}(r, R, \theta)$ with total energy E associated with a dissociative electronic state f of I_2. The EP rate is then given by

$$k_{\mathrm{EP}}^{v'nf} = \frac{2\pi}{\hbar}|\langle\phi_{v'}(r)\phi_{nv'}(R,\theta)|V_{\mathrm{c}}(r,R,\theta)|\phi_{Ef}(r,R,\theta)\rangle|^2 \tag{8}$$

where $V_{\mathrm{c}}(r, R, \theta)$ is the coupling matrix element between the B state and the final repulsive state, and E is the same energy as that of the quasi-bound state. This equation has been the basis for different approximations. The first one considered the slow Ar as a spectator in the dissociation process: the R and θ variables are set at their equilibrium values. The predissociation rate is then proportional to the B–f Franck–Condon factors of the I_2 molecule. This simple model has been tested for the $B''\,1_u$ and a 1_g repulsive states (Roncero *et al.* 1994a). For the $B''\,1_u$ state, the oscillations of the EP rate as a function of vibrational excitation are much slower than the experimental results (Burke and Klemperer 1993a). This is because the short-range repulsive portions of the B and B'' curves are very close and almost parallel; see figure 1. For the a 1_g state, the oscillatory pattern is reproduced fairly well (see figure 12), provided that the I_2 potential curves are shifted by a constant energy correction due to the Ar–I_2 interaction. Modified Franck–Condon simulations taking into account the possibility of vibrational energy transfer due to VP and using the IDIM PT1 PES for all the states involved were later conducted (Buchachenko 1998). They showed that the a 1_g and $1\,2_g$ states also produce oscillatory patterns for the EP rate which are close to the experimental ones (Burke and Klemperer 1993a), casting some doubt on the identification of the a 1_g state as the one responsible for the EP process.

One step beyond the spectator model consists in including the motion of the Ar atom in the dynamical treatment. Since the double continuum wavefunction $\phi_{Ef}(r, R, \theta)$ corresponding to the three-body break-up is quite difficult to compute, it is more convenient to obtain the EP rate from a time-dependent wavepacket calculation. In the time-dependent golden rule formalism, the EP rate is given by (Villarreal *et al.* 1991)

$$k_{\mathrm{EP}}^{v'nf} = \frac{1}{\hbar^2}\int_{-\infty}^{+\infty} \mathrm{d}t\, \mathrm{e}^{\mathrm{i}Et/\hbar}\langle\Phi_{v'nf}(r,R,\theta,t=0)|\Phi_{v'nf}(r,R,\theta,t)\rangle, \tag{9}$$

where the time-dependent wavepacket $\Phi_{v'n}(r, R, \theta, t)$ is propagated on the final dissociative surface f from the initial condition: $\Phi_{v'nf}(r, R, \theta, t = 0) = V_{\mathrm{c}}(r, R, \theta)\phi_{v'}(r)\phi_{nv'}(R, \theta)$. Two-dimensional fixed θ (Roncero *et al.* 1994b) and full three-dimensional time-dependent golden rule (Roncero *et al.* 1996) calculations both gave oscillations of the EP rate with v' which had the same period as the experimental ones if a 1_g was the final dissociative state. A good agreement with the absolute position of the oscillations was obtained with a van der Waals well of $100\,\mathrm{cm}^{-1}$ on the a 1_g PES, and the absolute values of the EP rates were in good agreement with the experimental ones for an interstate B–a coupling of the order of $14\,\mathrm{cm}^{-1}$.

The golden rule treatments of EP are perturbative models assuming that the VP process which occurs on the B electronic potential energy surface is not affected by the competing electronically non-adiabatic process. The competition between EP

and VP, which are of similar efficiency for $12 < v' < 26$, may induce non-perturbative effects. For instance, one may suppose that the broadening of the resonant bright and dark states due to electronic coupling may influence the IVR process. Thus, several attempts were made to study VP and EP simultaneously. The first approach (Buchachenko 1998) used classical dynamics to describe VP and surface hopping (with Landau–Zener probabilities) localized at crossing seams between electronic potentials to describe EP. This study was done on IDIM PT1 PESs (see section 3.4) and showed that all the final electronic states coupled to the B one contribute to EP. However, this model did not reproduce the oscillations in the VP efficiencies observed by Burke and Klemperer (1993a). Bastida *et al.* (1999) used a quantum description of the I_2 vibration and a classical description of the van der Waals modes for the VP process. The EP process was described by surface hopping, the probability being given by Franck–Condon factors. The potentials used were taken from Roncero *et al.* (1996). This model produced a good agreement with the experimental VPE. In addition, it was shown that first-order rate equations are not adequate to describe the time dependence of product populations. This was due to the dependence of the EP rate on the vibrational quantum numbers of the intermediate states of the process.

More recently, a full global quantum model including simultaneously the VP and EP processes was built using the DIM PT1 model for the B and the four coupled electronic states involved, $a\,1_g$, $a'\,0_g^+$, $B''\,1_u$ and $1\,2_g$ (Lepetit *et al.* 2002). In agreement with Buchachenko (1998), it was shown that all the dissociative electronic channels except $B''\,1_u$ could contribute significantly to EP. The total predissociation rates obtained for $v' = 18$ and 21 were in very good agreement with the real-time measurements of Zewail and coworkers (Breen *et al.* 1990, Willberg *et al.* 1992) (see figure 13). The calculated VPE oscillations were similar to the experimental ones, without any adjustment of the potentials. However, according to these calculations, the main source of oscillations comes from the VP rate, which is strongly influenced by IVR in the sparse limit. The EP rate is a rather smooth function of vibrational excitation. Indeed, each I_2 electronic repulsive state produces a partial EP rate which oscillates strongly according to its Franck–Condon factors to the B state. However, the oscillations of each of the three contributing electronic states are out of phase, so that the total EP rate is much smoother than each of its three contributions.

Lepetit *et al.* (2002) also studied the EP of the linear isomer at the same level of theory. The distinct nature of the VP process makes the EP mechanism for the linear isomer different from that of the T-shaped one. VP of the linear isomer is impulsive and fast, so that the argon atom rapidly leaves the interaction region without making large excursions out of the region of the collinear arrangement. Thus, EP has a lower probability and, in contrast to the T-shaped case, it proceeds almost exclusively through the $a'\,0_g^+$ state which is the only one coupled to the B state in the linear geometry. It would be nice to obtain experimental confirmation of this mechanism.

To summarize the situation on the EP and VP of $Ar\cdots I_2$, it must be admitted that after more than two decades of intense studies there is not yet a clear consensus on the following.

- Which are the I_2 electronic states responsible for EP: the single $a\,1_g$ state or a collaborative effect of several repulsive states?

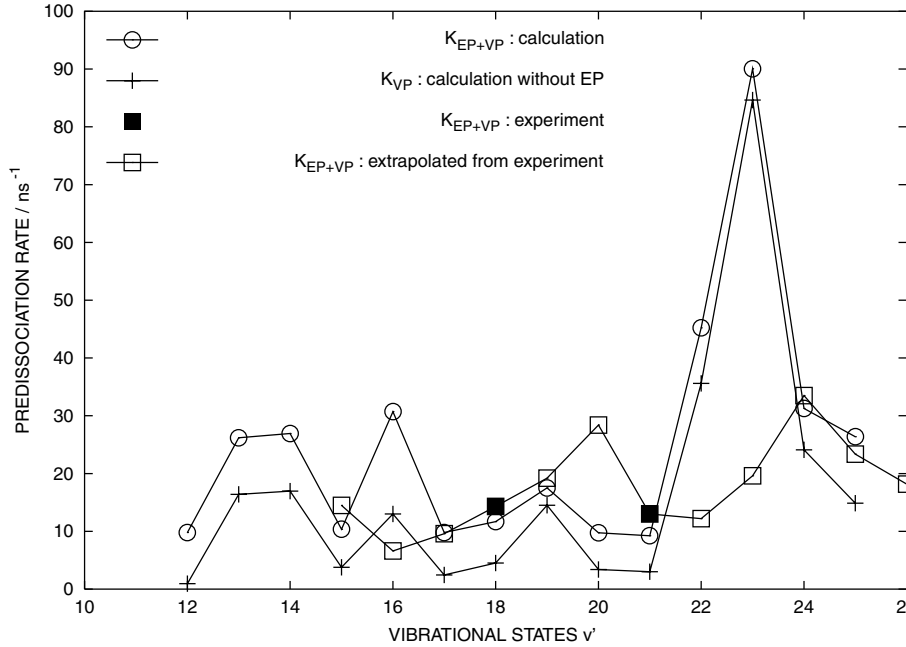

Figure 13. Predissociation rates (in ns^{-1}) as a function of the initial vibrational excitation v', for the ground van der Waals level. Two results from three-dimensional wave packet calculations are shown: k_{EP+VP}: full calculation, where the $B(^3\Pi 0_u^+)$ PES is coupled to the four dissociative states $B''\,1_u$, $a\,1_g$, $a'\,0_g^+$ and $1\,2g$. k_{VP}: only the $B(^3\Pi 0_g^+)$ state is included in the calculation, EP cannot take place. Also shown is the experimental total rate from Burke Klemperer (1993a). This rate has been extrapolated from VPEs by assuming a quasi-linear dependence of k_{VP} as a function of v'. Only the $v' = 18$ and 21 rates result from direct measurements (Breen *et al.* 1990, Willberg *et al.* 1992). (Reprinted from Lepetit *et al.* (2002).

- What is the origin of the VPE oscillations as a function a vibrational excitation: Franck–Condon factors inducing oscillations in the EP rates or sparse limit IVR inducing oscillations in the VP rates?

One way to solve this puzzle definitively would be to undertake measurements of the individual EP and VP rates, and not only of the VPE, which is now well established. This could be achieved by high-resolution spectroscopy or by real-time measurements, limited so far to two vibrational excitations.

7. Conclusions and perspectives

At the end of this review, it appears clearly that, although much progress has been made in the comprehension of the dynamical processes for the $Ar\cdots I_2$ van der Waals complex, much is still awaiting to be learned. There is nowadays little doubt that two isomers of the complex can coexist and that the linear isomer is responsible for the cage effect on I_2. There is little uncertainty about the dissociation energy of the T-shaped isomer. However, no clear consensus has been found yet on the energy of the linear isomer, and *ab initio* calculations have not yet reached a sufficient accuracy in the determination of these dissociation energies to decide whether the linear or the T-shaped isomer is the more bound one. Excitation of the perpendicular isomer to the B state produces long-lived resonance states and sharp lines in

photodissociation spectra. Excitation of the linear isomer leads to a fast dissociation dynamics and a broad background on the spectra. It is well established that the dissociation of the T-shaped isomer implies the loss of several vibrational quanta for I_2, and that it occurs as a stepwise IVR process. However, there is no final agreement on the regime of this process: sparse, as obtained by all quantum calculations, or statistical? EP is clearly the result of couplings between the B state and dissociative states induced by the presence of the Ar atom, but which dissociative state(s)? There is a consensus that there is a competition between EP and VP, which induces oscillations as a function of vibrational excitation in the relative efficiencies of these processes. However, what is the process responsible for these oscillations? One tentative interpretation is that the B state is coupled to the a 1_g dissociative one and that oscillations appear in the EP rate as a result of varying Franck–Condon factors. Another competing explanation is that the B state is coupled to a set of several dissociative states and that oscillations appear in the VP rate as a result of IVR in the sparse regime.

So what should be done to achieve complete understanding of this prototype system? On the theoretical side, priority should be put on the production of high-quality potentials. From the *ab initio* point of view, the most important steps to be taken next would be the explicit treatment of the SO interaction and the calculations of excited electronic states (first of all, the B one) and couplings. These steps are quite demanding and will require switching to another strategy—from the single-reference coupled cluster method, which is the method of choice for the ground state owing to its inherent ability to determine intermolecular interactions accurately, to multi-configurational methods which must carefully take into account intramolecular interactions describing the internal structure of the monomer. Both effects are equally important for the excited $Ar\cdots I_2$ system, and it may well be that *ab initio* methods capable of achieving a precise description are yet to be developed. The refinement of the DIM approach will require the use of an extended basis of atomic states covering the interaction with the ion-pair states and valence-excited manifolds of the molecular halogen. These new highly accurate potentials should be the starting points of dynamical calculations, the accuracy of which is nowadays only limited by the one of the electronic potentials. On the experimental side, it is striking to note that, although intense studies have been performed over decades, little is known on absolute values of total (EP + VP) decay rates as a function of initial excitation, whereas relative efficiencies of EP versus VP are well established. These total decay rates would bring much light on two open questions: one on the IVR regime (sparse/statistical) for VP, the other on the EP/VP competition (are oscillations on relative efficiencies induced by similar ones on EP or on VP?).

Another interesting perspective is to move to higher excitation energies above the valence manifold of the $Ar\cdots I_2$ complex. Theoretical studies of the Rydberg states converging to the positive ion threshold and studies of the cation itself in connection with experiments by Donovan's group (Cockett *et al.* 1993, 1994, Goode *et al.* 1994, Cockett *et al.* 1996) may provide additional precise information on the energetics of the complex in the ground state. Another challenging subject is the study of the $Ar\cdots I_2$ complex excited to ion-pair states accessible via single- or multi-photon transitions (Brand and Hoy 1987, Lawley and Donovan 1993). As follows from numerous collisional studies (Lawley 1988, Urbachs *et al.* 1993, Akopyan *et al.* 1999, Teule *et al.* 1999, Akopyan *et al.* 2001, Fecko *et al.* 2001, Bibinov *et al.* 2002, Fecko *et al.* 2002), interaction with a rare gas atom induces efficient non-adiabatic vibronic

transitions between closely lying states of distinct symmetry. This implies that, in the complex, EP (to bound I_2 electronic states in this case) will compete with vibrational predissociation. The proofs for such expectations can be found in the experimental study of large argon clusters (Fei *et al.* 1992). Recent calculations of the diabatic PESs and couplings in the frame of DIM models similar to those described here for valence states (Batista and Cocker 1997, Tscherbul *et al.* 2002) provide the grounds for future theoretical studies of the dynamics.

Acknowledgments

We owe much from numerous discussions with active researchers in this field over the past decades. It is not possible to mention all of them, but we wish to acknowledge fruitful interactions with J.A. Beswick, M.C. Heaven, K.C. Janda, W. Klemperer and C. Meier. We also wish to acknowledge financial support which, over the past few years, allowed us to interact closely and made the present work possible: INTAS 97-31573 and PICASSO HF1999-0132 international grants, national funding from Russian Foundation for Basic Research (grant 02-03-32676), Ministerio de Ciencia y Tecnología (grant BFM2001-2179) and CNRS. Allocation of CPU time from the Institut du Développement et des Ressources Informatiques is also gratefully acknowledged.

Appendix 1: Details of the DIM method to determine the $Ar\cdots I_2$ PES and couplings

The grounds of the DIM method are well described in the literature (e.g. Tully 1977, Kuntz 1979, 1982). It can be implemented in a variety of ways. Here the particular formulation relevant to the $Ar\cdots I_2$ complex is presented.

The total electronic Born–Oppenheimer Hamiltonian is expressed as a sum of the Hamiltonians corresponding to diatomic and atomic fragments of the system:

$$\hat{H} = \hat{H}_{I_2} + \hat{H}_{ArI_a} + \hat{H}_{ArI_b} - \hat{H}_{I_a} - \hat{H}_{I_b} - \hat{H}_{Ar}, \tag{10}$$

where 'a' and 'b' label iodine atoms. It can be recast into two terms, $\hat{H}_0$ describing the isolated fragments and $\hat{H}_1$ their interaction:

$$\hat{H}_0 = \hat{H}_{I_2} + \hat{H}_{Ar}, \tag{11}$$

$$\hat{H}_1 = \hat{H}_{1a} + \hat{H}_{1b} = (\hat{H}_{ArI_a} - \hat{H}_{I_a} - \hat{H}_{Ar}) + (\hat{H}_{ArI_b} - \hat{H}_{I_b} - \hat{H}_{Ar}). \tag{12}$$

The conventional DIM approach implies the variational solution of the Schrödinger equation for the total Hamiltonian, whereas the DIM perturbation theory approximation suggested independently by Naumkin (1991) and by Buchachenko and Stepanov (1996b) treats $\hat{H}_1$ in equation (12) as a perturbation.

The main feature of the DIM approach is the use of polyatomic basis functions (PBFs) constructed as linear combinations of many-electron functions centred on each atom and describing atomic states which contribute to the electronic configuration of the whole system. A minimum set of 36 PBF's can be defined as

$$\phi_k = \phi_{a_i b_j} = \chi^{Ar}\chi_i^a\chi_j^b. \tag{13}$$

It includes six SO functions describing the ^2P multiplet centred on each I atom $\chi_i^\alpha, \alpha = a, b$ and one function χ^{Ar} describing the ^1S state of Ar. This PBF set is assumed to form an orthonormal basis. Two attempts to take into account the

contribution from higher ion-pair states of the iodine gave controversial results (Grigorenko *et al.* 1997a, Naumkin and McCourt 1996b).

Using the basis set ϕ_k of equation (13), it is easy to evaluate the matrix elements of the diatomic fragment Hamiltonians contributing to $\hat{\boldsymbol{H}}_1$ in equation (12). In the reference frame related to the I_α–Ar axis $\mathcal{R}_\alpha$, the $\hat{\boldsymbol{H}}_{ArI_\alpha}$ matrix has a particularly simple form and is parametrized by the non-relativistic V_Σ and V_Π potentials of the $Ar \cdots I$ molecule in its $^2\Sigma^+$ and $^2\Pi$ state respectively. It is convenient to choose the I_2 axis **r** as the common reference frame. The transformation from the $\mathcal{R}_\alpha$ to the **r** frame is given by the standard rotation matrices $\mathbf{D}_\alpha(0, \beta_\alpha, 0)$ (Wigner rotation matrices or direction cosine matrices, depending on the particular choice of atomic basis functions) in which only one angle β_α is non-zero.

Constructing the $\hat{\boldsymbol{H}}_0$ matrix in the PBF set is more involved owing to the complexity of the I_2 electronic structure. Its eigenfunctions

$$\hat{\boldsymbol{H}}_0 \, \psi_n = u_n \, \psi_n, \tag{14}$$

where n enumerates the adiabatic electronic states of I_2 and u_n are the corresponding energies as a function of r, are expressed in terms of the PBF

$$\psi_n(r) = \sum_k C_k^n(r) \phi_k. \tag{15}$$

The total Hamiltonian matrix is therefore

$$\mathbf{H} = \mathbf{u} + \mathbf{C}^\dagger \left(\mathbf{D}_\mathrm{a}^\dagger \mathbf{H}_{ArI_\mathrm{a}} \mathbf{D}_\mathrm{a} + \mathbf{D}_\mathrm{b}^\dagger \mathbf{H}_{ArI_\mathrm{b}} \mathbf{D}_\mathrm{b} - \mathbf{H}_{I_\mathrm{a}} - \mathbf{H}_{I_\mathrm{b}} \right) \mathbf{C}, \tag{16}$$

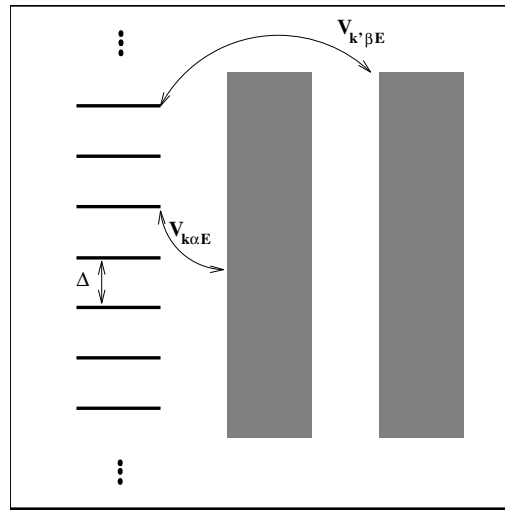

Figure 14. Energy diagram and couplings of the simplified analytical model for the classification of IVR regimes. Zero-order bound states are coupled together by a constant value V. One of them is the bright state and can be populated by photoexcitation, the others are dark states. We assume that diagonalization of this zero-order Hamiltonian provides first-order eigenstates with equidistant eigenenergies separated by $i\Delta$. These eigenstates are coupled to the α and β continua, which gives them some width Γ which is assumed to be constant. (Reprinted from Roncero *et al.* (1997).)

where **u** is a diagonal matrix containing the energy curves of I_2 and $\mathbf{H}_{I_\alpha}$ are diagonal matrices containing the energies of the atomic iodine terms (vanishing in the non-relativistic case).

The different DIM approaches correspond to different representations of the atomic basis functions, to different approximations for the eigenfunctions of $\hat{H}_0$ (equations (11) and (15)), and to two different ways of treating $\hat{H}_1$ (equation (11) and the second term of the sum in equation (16)): exactly or as a perturbation. These approaches are discussed in section 3.4.

Appendix 2: classification of IVR regimes

The different regimes of IVR, from sparse to statistical, can be modelled in terms of an infinite collection of non-interacting bound states (see figure 14), with energies $E_n = n\Delta$, $n = -\infty, \ldots, \infty$, coupled to a dissociative continuum, so that their half-width is equal to Γ for each of them (Roncero *et al.* 1997), in close correspondence to the treatment of Bixon and Jortner (1969). It can be considered that this ensemble of first-order bound states arises from the diagonalization of an initial zero-order 'bright' state coupled (by a constant quantity V) to an infinite ensemble of zero-order 'dark' states. Therefore, the initial wavepacket can be expanded in terms of these states with a weight ratio $a_n/a_0 = V/(n\Delta - i\Gamma)$ (Roncero *et al.* 1997). This model

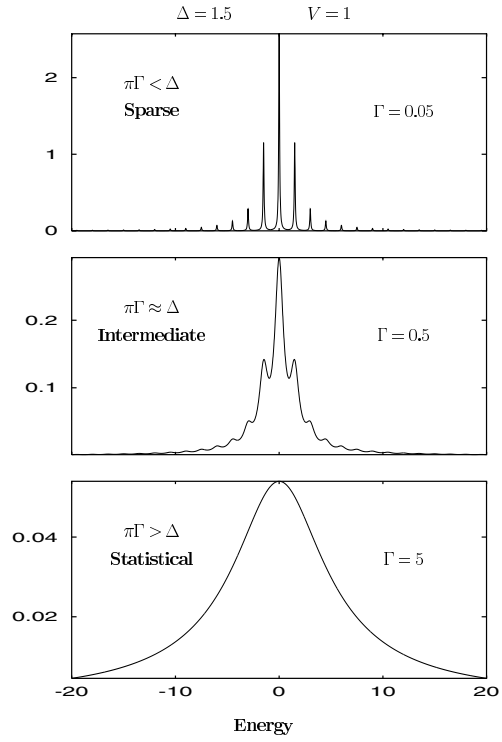

Figure 15. Spectra corresponding to the situation described in figure 14. The coupling between zero-order states is fixed to $V = 1$, and the spacing between first-order states is $\Delta = 1.5$. One gradually moves from sparse to intermediate and then to statistical IVR regimes as the coupling strength of the first-order states to the continuum is increased from $\Gamma = 0.05$ to 0.5 and then 5. (Reprinted from Roncero *et al.* (1997).)

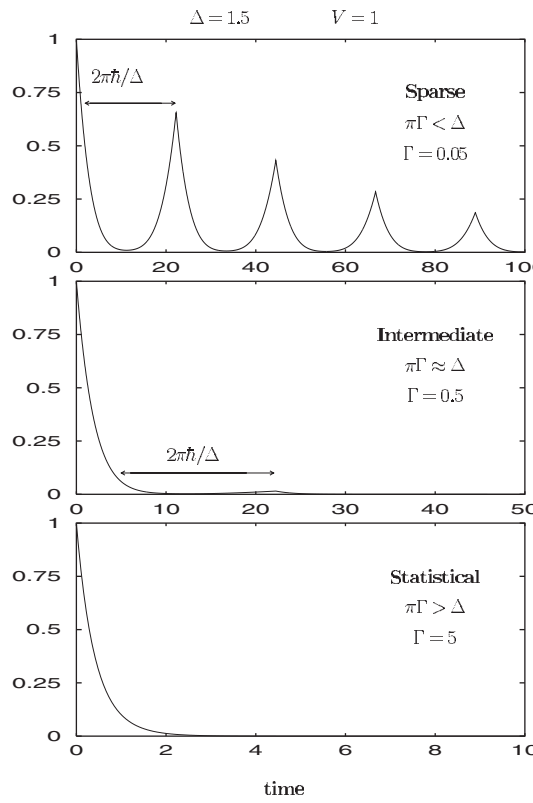

Figure 16. Time evolution of the initial state (zero-order bright state) for the three IVR regimes of figure 15. (Reprinted from Roncero *et al.* (1997).)

leads to a natural classification, as previously discussed (Bixon and Jortner 1969, Freed and Nitzan 1980, Miller 1991, Uzer 1991), of IVR dynamics in terms of the Γ/Δ ratio as follows.

(1) *Sparse regime*, ($\Gamma \ll \Delta$). The resonances are well separated (see figures 15 and 16). The initially populated bright state will usually interact with one or a few dark states, so that quantum phenomena such as recurrences are readily apparent. In some cases, the zero-order bound states are indirectly coupled through their mutual coupling to the dissociative continua (Roncero *et al.* 1993, Roncero and Gray 1996, Roncero *et al.* 1997).

(2) *Intermediate regime* ($\Gamma \approx \Delta$). In this regime the resonances are mixed but have not completely lost their individual identity (see figures 15 and 16). This will be apparent both in the spectrum, in which nearby transitions will overlap with each other, and in the dynamics, which will exhibit non-exponential decay with weak recurrences in the population of the initially excited state.

(3) *Statistical regime* ($\Gamma \gg \Delta$). In this regime there are so many closely spaced resonances that they blend together to yield a quasi-Lorentzian excitation spectrum. As a consequence, the initial states lose their identity and decay irreversibly as a single exponential.

In the sparse and intermediate regimes the VP rate is expected to oscillate as a function of v' (except if there is a smoothing out due to averaging as will be commented on below), and the only regime in which a smooth monotonic behaviour is expected is the statistical one. This regime is traditionally attributed to large molecules and it is interesting to know whether it can occur in such small molecular systems.

The statistical limit can be obtained by increasing the density of states (*i.e.* decreasing the spacing Δ) and/or the width of each individual state, Γ, but also by varying the total energy spreading of the spectrum, which depends enormously on the initial state.

References

Akopyan, M. E., Bibinov, N. R., Kokh, D. B., Pravilov, A. M., Stepanov, M. B., and Vasyutinskii, O. S., 1999, *Chem. Phys.*, **242**, 263.

Akopyan, M. E., Bibinov, N. K., Kokh, D. B., Pravilov, A. M., Sharova, O. L., and Stepanov, M. B., 2001, *Chem. Phys.*, **263**, 459.

Alfano, J. C., Kliner, D., Johnson, A. E., Levinger, N. E., and Barbara, P. F., 1992, in *Ultrafast Phenomena VIII*, edited by J. L. Martin, A. Migus, G. A. Mourou and A. H. Zewail (New York: Springer), p. 653.

Apkarian, V. A., and Schwentner, N., 1999, *Chem. Rev.*, **99**, 1481.

Aquilanti, V., Luzzatti, E., Pirani, F., and Volpi, G. G., 1988, *J. chem. Phys.*, **89**, 6165.

Aquilanti, V., Candori, R., Cappelletti, D., Luzzatti, E., and Pirani, F., 1990, *Chem. Phys.*, **145**, 293.

Aquilanti, V., Cappelletti, D., Lorent, V., Luzzatti, E., and Pirani, F., 1993, *J. phys Chem.*, **97**, 2063.

Arnot, C., and McDowell, C., 1958, *Can. J. Chem.*, **36**, 114.

Asmis, K. R., Taylor, T. R., Xu, C., and Neumark, D. M., 1998, *J. chem. Phys.*, **109**, 4389.

Baba, H., and Sakurai, K., 1985, *J. chem. Phys.*, **82**, 4977.

Bastida, A., Zúñiga, J., Requena, A., Sola, I., Halberstadt, N., and Beswick, J. A., 1997, *Chem. Phys. Lett.*, **280**, 185.

Bastida, A., Zúñiga, J., Requena, A., Halberstadt, N., and Beswick, J. A., 1999, *Chem. Phys.*, **240**, 229.

Bastida, A., Zúñiga, J., Requena, A., Miguel, B., Beswick, H. A., Vigué, J., and Halberstadt, N., 2002, *J. chem. Phys.*, **116**, 1944.

Batista, V. S., and Coker, D. F., 1996, *J. chem. Phys.*, **105**, 4033; 1997, *J. chem. Phys.*, **106**, 6923.

Baumfalk, R., Nahler, N. H., and Buck, U., 2001, *Faraday Discuss.*, **118**, 247.

Becker, C. H., Casavecchia, P., and Lee. Y. T., 1979, *J. chem. Phys.*, **70**, 2986.

Beeken, P. B., Hanson, E. A., and Flynn, G. W., 1983, *J. chem. Phys.*, **78**, 5892.

Benderskii, A. V., Zadoyan, R., and Apkarian, V. A., 1997, *J. chem. Phys.*, **107**, 8437.

Ben-Nun, M., Levine, R. D., Jonas, D. M., and Fleming, G. R., 1995, *Chem. Phys. Lett.*, **245**, 629.

Beswick, J. A., and Jortner, J., 1977, *Chem. Phys. Lett.*, **49**, 13; 1978a, *J. chem. Phys.*, **69**, 512; 1978b, *J. chem. Phys.*, **68**, 2277; 1980, *Mol. Phys.*, **39**, 1137; 1981, *Adv. chem. Phys.*, **47**, 363.

Beswick, J. A., Delgado-Barrio, G., and Jortner, J., 1979, *J. chem. Phys.*, **70**, 3895.

Beswick, J. A., Monot, R., Philippoz, J., and van den Bergh, H., 1987, *J. chem. Phys.*, **86**, 3965.

Bibinov, N. R., Malinina, O. L., Pravilov, A. M., Stepanov, M. B., and Zakharova, A. A., 2002, *Chem. Phys.*, **277**, 179.

Bixon, M., and Jortner, J., 1969, *J. chem. Phys.*, **50**, 3284.

Blazy, J. A., DeKoven, B. M., Russell, T. D., and Levy, D. H., 1980, *J. chem. Phys.*, **72**, 2439.

Borrmann, A., Li, Z., and Martens, C. C., 1993, *J. chem. Phys.*, **98**, 8514.
Brand, J. C. D., and Hoy, A. R., 1987, *Appl. Spectrosc. Rev.*, **23**, 285.
Breen, J. J., Willberg, D. M., Gutmann, M., and Zewail, A. H., 1990, *J. chem. Phys.*, **93**, 9180.
Brown, F. B., Schwenke, D. W., and Truhlar, D. G., 1985, *Theor. Chim. Acta*, **68**, 23.
Brown, R. L., and Klemperer, W., 1964, *J. chem. Phys.*, **41**, 3072.
Broyer, M., Vigué, J., and Lehmann, J. C., 1975, *J. chem. Phys.*, **63**, 5428; 1976, *J. chem. Phys.*, **64**, 4793.
Buchachenko, A. A., 1998, *Chem. Phys. Lett.*, **292**, 273.
Buchachenko, A. A., and Stepanov, N. F., 1993, *J. chem. Phys.*, **98**, 5486; 1996a, *Chem. Phys. Lett.*, **261**, 591; 1996b, *J. chem. Phys.*, **104**, 9913; 1997a, *J. chem. Phys.*, **106**, 4358; 1997b, *J. chem. Phys.*, **106**, 10134; 1998a, *Russ. J. phys. Chem.*, **72**, 69; 1998b, *Russ. J. phys. Chem.*, **72**, 390.
Buchachenko, A. A., González-Lezana, T., Hernández, M. I., Delgado-Barrio, G., and Villarreal, P., 2000a, *Chem. Phys. Lett.*, **318**, 578.
Buchachenko, A. A., Roncero, O., and Stepanov, N. F., 2000b, *Russ. J. chem. Phys.*, **74** (Suppl.2), S193.
Buchachenko, A. A., Krems, R. V., Szczęśniak, M. M., Xiao, Y.-D., Viehland, L. A., and Chałasiński, G., 2001, *J. chem. Phys.*, **114**, 9919.
Buchachenko, A. A., Prosmiti, R., Cunha, C., Delgado-Barrio, G., and Villarreal, P., 2002, *J. chem. Phys.*, **117**, 6117.
Burcl, R., Krems, R. V., Buchachenko, A. A., Szczęśniak, M. M., Chałasiński, G., and Cybulski, S. M., 1998, *J. chem. Phys.*, **109**, 2144.
Burde, D. H., McFarlane, R. A., and Wiesenfeld, J. R., 1974, *Phys. Rev.* A, **10**, 1917.
Burke, M. L., and Klemperer, W., 1993a, *J. chem. Phys.*, **98**, 6642; 1993b, *J. chem. Phys.*, **98**, 1797.
Burroughs, A., and Heaven, M. C., 2001, *J. chem. Phys.*, **114**, 7027.
Burroughs, A., van Marter, T., and Heaven, M. C., 1999, *J. chem. Phys.*, **111**, 2478.
Burroughs, A., Kerenskaya, G., and Heaven, M. C., 2001, *J. chem. Phys.*, **115**, 784.
Capelle, G. A., and Broida, H. P., 1973, *J. chem. Phys.*, **58**, 4212.
Casavecchia, P., He, G., Sparks, R., and Lee, Y. T., 1982, *J. chem. Phys.*, **77**, 1878.
Castleman, A. W. Jr., 1992, in *Clusters of Atoms and Molecules*, edited by H. Haberland (New York: Springer).
Chałasiński, G., and Szczęśniak, M. M., 1994, *Chem. Rev.*, **94**, 1723.
Chałasiński, G., Gutowski, M., Szczęśniak, M. M., Sadlej, J., and Scheiner, S., 1994, *J. chem. Phys.*, **101**, 6800.
Chergui, M., and Schwentner, N., 1992, *Trends chem. Phys.*, **2**, 89.
Cline, J. I., Evard, D. D., Reid, B. P., Sivakumar, N., Thommen, F., and Janda, K. C., 1987, in *Structure and Dynamics of Weakly-Bound Molecular Systems*, edited by A. Weber (Dordrecht: Reidel), p. 533.
Cockett, M., Goode, J. G., Lawley, K. P., and Donovan, R. J., 1993, *Chem. Phys. Lett.*, **214**, 27.
Cockett, M., Goode, J. G., Maier, R. R. J., Lawley, K. P., and Donovan, R. J., 1994, *J. chem. Phys.*, **101**, 126.
Cockett, M., Beattie, D. A., Donovan, R. J., and Lawley, K. P., 1996, *Chem. Phys. Lett.*, **259**, 554.
Conley, A. J., Fang, J.-Y., and Martens, C. C., 1997, *Chem. Phys. Lett.*, **272**, 103.
Cybulski, S. M., and Holt, J. S., 1999, *J. chem. Phys.*, **110**, 7745.
Cybulski, S. M., Burcl, R., Chałasiński, G., and Szczęśniak, M. M., 1995, *J. chem. Phys.*, **103**, 10116.
Dalby, F. W., Levy, C., and Vanderlinde, J., 1984, *Chem. Phys.*, **85**, 23.
de Jong, W. A., Visscher, L., and Nieuwpoort, W. C., 1997, *J. chem. Phys.*, **107**, 9046.
Delaney, N., Faeder, J., and Parson, R., 1999, *J. chem. Phys.*, **111**, 651.
Delgado-Barrio, G., Villarreal, P., Mareca, P., and Albelda, G., 1983, *J. chem. Phys.*, **78**, 280.
Derouard, J., and Sadeghi, N., 1984a, *Chem. Phys.*, **88**, 171; 1984b, *J. chem. Phys.*, **81**, 3002.

Dexheimer, S. L., Durand, M., Brunner, T. A., and Prtichard, D. E., 1982, *J. chem. Phys.*, **76**, 4996.
Dexheimer, S. L., Brunner, T. A., and Pritchard, D. E., 1983, *J. chem. Phys.*, **79**, 5206.
Drabe, K. E., and van Voorst, J. D. W., 1985, *Chem. Phys.*, **99**, 135.
Drabe, K. E., de Groot, A., and van Voorst, J. D. W., 1985a, *Chem. Phys.*, **99**, 121.
Drabe, K. E., Langelaar, J., Bebelaar, D., and van Voorst, J. D. W., 1985b, *Chem. Phys.*, **97**, 411.
Du, H., Krajnovich, D. J., and Parmenter, C. S., 1991, *J. chem. Phys.*, **95**, 2104.
Evard, D. D., Thommen, F., and Janda, K. C., 1986, *J. chem. Phys.*, **84**, 3630.
Evard, D. D., Bieler, C. R., Cline, J. I., Sivakumar, N., and Janda, K. C., 1988a, *J. chem Phys.*, **89**, 2829.
Evard, D. D., Cline, J. I., and Janda, K. C., 1988b, *J. chem. Phys.*, **88**, 5433.
Ewing, G. E., 1979, *J. chem. Phys.*, **71**, 3143; 1980, *J. chem. Phys.*, **72**, 2096; 1982, *Faraday Discuss. Chem. Soc.*, **73**, 402; 1986, *J. phys. Chem.*, **90**, 1990.
Fang, J., and Martens, C. C., 1996, *J. chem. Phys.*, **105**, 9072.
Fecko, C. J., Freedman, M. A., and Stephenson, T. A., 2001, *J. chem. Phys.*, **115**, 4132; 2002, *J. chem. Phys.*, **116**, 1361.
Fei, S., Zheng, X., Heaven, M. C., and Tellinghuisen, J., 1992, *J. chem. Phys.*, **97**, 6057.
Franck, J., and Rabinovitch, E., 1934, *Trans. Faraday Soc.*, **30**, 120.
Franck, J., and Wood, R. W., 1911, *Philos. Mag.*, Ser. 6, **21**, 314.
Freed, K., and Nitzan, A., 1980, *J. chem. Phys.*, **73**, 4765.
Gardner, D. J., and Preston, S. R., 1992, *J. chem. eng. Data*, **37**, 500.
Gentry, W. R., 1984, *J. chem. Phys.*, **81**, 5737.
Gerber, R. B., McCoy, A. B., and Garcia-Vela, A., 1994, *Annu. Rev. phys. Chem.*, **45**, 275.
Gersonde, I. H., and Gabriel, H., 1993, *J. chem. Phys.*, **98**, 2094.
Gerstenkorn, S., and Luc, P., 1985, *J. Phys.* (Paris), **46**, 865.
Goldfield, E. M., and Gray, S. K., 1997a, *J. Chem. Soc. Faraday Trans.*, **93**, 909; 1997b, *Chem. Phys Lett.*, **276**, 1.
Goldstein, N., Brack, T. L., and Atkinson, G. H., 1986, *J. chem. Phys.*, **85**, 2684.
González-Lezana, T., Hernández, M. I., Delgado-Barrio, G., Buchachenko, A. A., and Villarreal, P., 1996, *J. chem. Phys.*, **105**, 7454.
Goode, J. G., Cockett, M. C. R., Lawley, K. P., and Donovan, R. J., 1994, *Chem. Phys. Lett.*, **231**, 521.
Gray, S. K., 1992, *Chem. Phys. Lett.*, **197**, 86.
Gray, S. K., and Rice, S. A., 1986, *Faraday Discuss. Chem. Soc.*, **82**, 307.
Gray, S. K., and Roncero, O., 1995, *J. phys. Chem.*, **99**, 2512.
Gray, S. K., Rice, S. A., and Davis, M. J., 1986, *J. phys. Chem.*, **90**, 3470.
Greenblatt, B. J., Zanni, M. T., and Neumark, D. M., 1997, *Faraday Discuss.*, **108**, 101.
Grigorenko, B. L., Nemukhin, A. V., and Apkarian, V. A., 1997a, *Chem. Phys.*, **219**, 161.
Grigorenko, B. L., Nemukhin, A. V., Buchachenko, A. A., Stepanov, N. F., and Umanskii, S. Y., 1997b, *J. chem. Phys.*, **106**, 4575.
Halberstadt, N., and Beswick, J. A., 1982, *Faraday Discuss. Chem. Soc.*, **73**, 357.
Halberstadt, N., Beswick, J. A., Roncero, O., and Janda, K. C., 1992a, *J. chem. Phys.*, **96**, 2404.
Halberstadt, N., Serna, S., Roncero, O., and Janda, K. C., 1992b, *J. chem. Phys.*, **97**, 341.
Hall, G., McAuliffe, M. J., Giese, C. F., and Gentry, W. R., 1983, *J. chem. Phys.*, **78**, 5260.
Harris, A. L., Brown, J. K., and Harris, C. B., 1988, *Annu. Rev. phys. Chem.*, **39**, 341.
Harris, S. J., Novick, S. E., Klemperer, W., and Falconer, W. E., 1974, *J. chem. Phys.*, **61**, 193.
Hernández, M. I., González-Lezana, T., Delgado-Barrio, G., Villarreal, P., and Buchachenko, A. A., 2000, *J. chem. Phys.*, **113**, 4620.
Hill, T., 1946, *J. chem. Phys.*, **14**, 465.
Hirschfelder, J. O., Curtiss, C. M., and Bird, R. B., editors, 1954, *Molecular Theory of Gases and Liquids*, 2nd Edn (New York: Wiley).

HU, X., and MARTENS, C. C., 1933a, *J. chem. Phys.*, **99**, 9532; 1993b, *J. phys. Chem.*, **98**, 8551.
HUANG, S. S., BIELDER, C. R., TAO, F.-M., KLEMPERER, W., CASAVECCHIA, P., VOLPI, G. G., JANDA, K. C., and HALBERSTADT, N., 1995, *J. chem. Phys.*, **102**, 8846.
HUBER, K. P., and HERZBERG, G., editors, 1979, *Molecular Spectra and Molecular Structure. IV. Constants of Diatomic Molecules* (New York: van Nostrand).
JAHN, D. G., CLEMENT, S. G., and JANDA, K. C., 1994, *J. chem. Phys.*, **101**, 283.
JAHN, D. G., BARNEY, W. S., CABALO, J., CLEMENT, S., SLOTTERBACK, T. J., JANDA, K. C., and HALBERSTADT, N., 1996, *J. chem. Phys.*, **104**, 3501.
JOHNSON, K. E., WHARTON, L., and LEVY, D. H., 1978, *J. chem. Phys.*, **69**, 2719.
JOHNSON, K. E., SHARFIN, W., and LEVY, D. H., 1981, *J. chem. Phys.*, **74**, 163.
JUNGWIRTH, P., FREDJ, E., and GERBER, R. B., 1996, *J. chem. Phys.*, **104**, 1.
KAJIMOTO, O., and FUENO, T., 1972, *Bull. Chem. Soc. Japan*, **45**, 99.
KATÔ, J., and BABA, M., 1995, *Chem. Rev.*, **95**, 2311.
KENNY, J. E., JOHNSON, K. E., SHARFIN, W., and LEVY, D. H., 1980a, *J. chem. Phys.*, **72**, 1109.
KENNY, J. E., RUSSELL, T. D., and LEVY, D. H., 1980b, *J. chem. Phys.*, **73**, 3607.
KITAIGORODSKII, A. I., 1951, *Izv. Akad. Nauk SSSR, Ser. Fiz.*, **15**, 157.
KLEMPERER, W., 2001, private communication.
KOKUBO, T., and FUJIMURA, Y., 1986, *J. chem. Phys.*, **85**, 7106.
KRAJNOVICH, D. J., BUTZ, K. W., DU, H., and PARMENTER, C. S., 1989a, *J. chem. Phys.*, **91**, 7705; 1989b, *J. chem. Phys.*, **91**, 7725.
KUBIAK, G., FITCH, P., WHARTON, L., and LEVY, D. H., 1978, *J. chem. Phys.*, **68**, 4477.
KUNTZ, P. J., 1979, in *Atom–Molecule Collision Theory*, edited by R. B. Bernstein (New York: Plenum), p. 79; 1982, *Ber. Bunsenges. phys. Chem.*, **86**, 367.
KUNZ, C. F., BURGHARDT, I., and HESS, B., 1998, *J. chem. Phys.*, **109**, 359.
KURZEL, R. B., and STEINFELD, J. I., 1970, *J. chem. Phys.*, **53**, 3293.
KURZEL, R. B., STEINFELD, J. I., HATZENBUHLER, D. A., and LEROI, G. E., 1971, *J. chem. Phys.*, **55**, 4822.
LARA-CASTELLS, M. P. D., KREMS, R. V., BUCHACHENKO, A. A., DELGADO-BARRIO, G., and VILLARREAL, P., 2001, *J. chem. Phys.*, **115**, 10438.
LAWLEY, K. P., 1988, *Chem. Phys.*, **127**, 363.
LAWLEY, K. P., and DONOVAN, R. J., 1993, *J. Chem. Soc. Faraday Trans.*, **89**, 1885.
LAWRENCE, W. G., VAN MARTER, T. A., NOWLIN, M. L., and HEAVEN, M. C., 1997, *J. chem. Phys.*, **106**, 127.
LENZER, T., FURLANETTO, M. R., ASMIS, K. R., and NEUMARK, D. M., 1998, *J. chem. Phys.*, **109**, 10754.
LENZER, T., YOURSHAW, I., FURLANETTO, M. R., REISER, G., and NEUMARK, D. M., 1999, *J. chem. Phys.*, **110**, 9578.
LEPETIT, B., RONCERO, O., BUCHACHENKO, A. A., and HALBERSTADT, N., 2002, *J. chem. Phys.*, **116**, 8367.
LEVY, D. H., 1981, *Adv. chem. Phys.*, **47**, 323.
LI, Z., ZADOYAN, R., APKARIAN, V. A., and MARTENS, C. C., 1995, *J. phys. Chem.*, **99**, 7453.
LIENAU, C., and ZEWAIL, A. H., 1994, *Chem. Phys. Lett.*, **222**, 224; 1996, *J. phys. Chem.*, **100**, 18629.
LIU, L., and GUO, H., 1995, *Chem. Phys. Lett.*, **237**, 299.
LIU, Q., WANG, J., and ZEWAIL, A. H., 1993, *Nature*, **364**, 427; 1995, *J. phys. Chem.*, **99**, 11321.
MA, Z., JONS, S. D., GIESE, C. F., and GENTRY, W. R., 1991, *J. chem. Phys.*, **94**, 8608.
MACLER, M., and HEAVEN, M. C., 1991, *Chem. Phys.*, **151**, 219.
MARTIN, F., BACIS, R., CHURASSY, S., and VERGÉS, J., 1986, *J. mol. Spectrosc.*, **116**, 71.
MEIER, C., ENGEL, V., and BESWICK, J., 1998, *Chem. Phys. Lett.*, **287**, 487.
MILLER, W. H., 1991, *Phys. Rep.*, **199**, 73.
MIRANDA, M. P., BESWICK, J. A., and HALBERSTADT, N., 1994, *Chem. Phys.*, **187**, 185.
MULLIKEN, R. S., 1957, *Phys. Rev.*, **57**, 500; 1971, *J. chem. Phys.*, **55**, 288.
NAKAGAWA, K., KITAMURA, M., SUZUKI, K., KONDOW, T., MUNAKATA, T., and KASUYA, T., 1986, *Chem. Phys.*, **106**, 259.

NAUMKIN, F. Y., 1991, *Sov. Phys. Lebedev Inst. Rep.* (USA), **8**, 27; 1998, *Chem. Phys.*, **226**, 319; 2001, *Chem. phys. Chem.* [*Angew. Chem.*, **40**], **2**, 121.
NAUMKIN, F. Y., and KNOWLES, P. J., 1995, *J. chem. Phys.*, **103**, 3392.
NAUMKIN, F. Y., and MCCOURT, F., 1997, *J. chem. Phys.*, **107**, 5702; 1998a, *J. chem. Phys.*, **108**, 9301; 1998b, *Chem. Phys. Lett.*, **292**, 63; 1998c, *Chem. Phys. Lett.*, **294**, 71; 1999, *Mol. Phys.*, **96**, 1043.
NOORBATCHA, I., RAFF, L. M., and THOMSON, D. L., 1984, *J. chem. Phys.*, **81**, 5658.
NOWLIN, M. L., and HEAVEN, M. C., 1993, *J. chem. Phys.*, **99**, 5654.
PAPANIKOLAS, J. M., VORSA, V., NADAL, M. E., CAMPAGNOLA, P. J., GORD, J. R., and LINEBERGER, W. C., 1992, *J. chem. Phys.*, **97**, 7002; 1993, *J. chem. Phys.*, **99**, 8733.
PARTRIDGE, H., STALLCOP, J. R., and LEVINE, E., *J. chem. Phys.*, **115**, 6471.
PAZYUK, E. A., STOLYAROV, A. V., PUPYSHEV, V. I., STEPANOV, N. F., UMANSKII, S. Y., and BUCHACHENKO, A. A., 2001, *Mol. Phys.*, **99**, 91.
PEDERSEN, D. B., and WEITZ, E., 2002, *J. chem. Phys.*, **116**, 9897.
PHILIPPOZ, J. M., MONOT, R., and VAN DEN BERGH, H., 1986, *Helv. Phys. Acta*, **58**, 1089.
PHILIPPOZ, J. M., VAN DEN BERGH, H., and MONOT, R., 1987, *J. phys. Chem.*, **91**, 2545.
PHILIPPOZ, J. M., MONOT, R., and VAN DEN BERGH, H., 1990, *J. chem. Phys.*, **92**, 288.
PROSMITI, R., CUNHA, C., VILLARREAL, P., and DELGADO-BARRIO, G., 2002a, *J. chem. Phys.*, **116**, 9249.
PROSMITI, R., VILLARREAL, P., and DELGADO-BARRIO, G., 2002b, *Chem. Phys. Lett.*, **359**, 473.
PROSMITI, R., VILLARREAL, P., DELGADO-BARRIO, G., and RONCERO, O., 2002c, *Chem. Phys Lett.*, **359**, 229.
ROCK, A. B., VAN ZOEREN, C. M., KABLE, S. H., EDVARDS, G. B., and KNIGHT, A. E. W., 1988, *J. chem. Phys.*, **89**, 6777.
ROHRBACHER, A., JANDA, K. C., VENEVENTI, L., CASAVECCHIA, P., and VOLPI, G. G., 1997a, *J. phys. Chem.* A, **101**, 6528.
ROHRBACHER, A., WILLIAMS, J., JANDA, K. C., CYBULSKI, S. M., BURCL, R., SZCZĘŚNIAK, M. M., CHAŁASIŃSKI, G., and HALBERSTADT, N., 1997b, *J. chem. Phys.*, **106**, 2685.
ROHRBACHER, A., RUCHTI, T., JANDA, K. C., BUCHACHENKO, A. A., HERNÁNDEZ, M. I., GONZÁLEZ-LEZANA, T., VILLARREAL, P., and DELGADO-BARRIO, G., 1999a, *J. chem. Phys.*, **110**, 256.
ROHRBACHER, A., WILLIAMS, J., and JANDA, K. C., 1999b, *Phys. Chem. chem. Phys.*, **1**, 5263.
RONCERO, O., and GRAY, S. K., 1996, *J. chem. Phys.*, **104**, 4999.
RONCERO, O., CAMPOS-MARTÍNEZ, J., CORTINA, A. M., VILLARREAL, P., and DELGADO-BARRIO, G., 1988, *Chem. Phys. Lett.*, **148**, 62.
RONCERO, O., VILLARREAL, P., DELGADO-BARRIO, G., HALBERSTADT, N., and JANDA, K. C., 1993, *J. chem. Phys.*, **99**, 1035.
RONCERO, O., HALBERSTADT, N., and BESWICK, J. A., 1994a, in *Reaction Dynamics in Clusters and Condensed Phases*, edited by J. Hortner, R. D. Levine and B. Pullmann (Dordrecht: Kluwer), p. 73; 1994b *Chem. Phys. Lett.*, **226**, 82; 1996, *J. chem. Phys.*, **104**, 7554.
RONCERO, O., CALOTO, D., JANDA, K. C., and HALBERSTADT, N., 1997, *J. chem. Phys.*, **107**, 1406.
RONCERO, O., CAMPOS-MARTÍNEZ, J., HERNÁNDEZ, M. I., DELGADO-BARRIO, G., VILLARREAL, P., and RUBAYO-SONEIRA, J., 2001a, *J. chem. Phys.*, **115**, 2566.
RONCERO, O., LEPETIT, B., BESWICK, J. A., HALBERSTADT, N., and BUCHACHENKO, A. A., 2001b, *J. chem. Phys.*, **115**, 6961.
RÖSSLER, F., 1935, *Z. Phys.*, **96**, 251.
RUBINSON, M., and STEINFELD, J. I., 1974, *Chem. Phys.*, **4**, 467.
RUBINSON, M., GARETZ, B., and STEINFELD, J. I., 1974, *J. chem. Phys.*, **60**, 3082.
SAENGER, K. L., MCCLELLAND, G. M., and HERSCHBACH, D. R., 1981, *J. phys. Chem.*, **85**, 3333.
SANOV, A., and LINEBERGER, W. C., 2002, *Phys. Chem. Comm.*, **5**, 165.
SCHEK, I., JORTNER, J., RAZ, T., and LEVINE, R. D., 1996, *Chem. Phys. Lett.*, **257**, 273.
SCHRÖDER, H., and GABRIEL, H., 1996, *J. chem. Phys.*, **104**, 587.

SCHROEDER, J., and TROE, J., 1987, *Annu. Rev. phys. Chem.*, **38**, 163.
SCHWARTZ, B. J., KING, J. C., ZHANG, J. Z., and HARRIS, C. B., 1993, *Chem. Phys. Lett.*, **203**, 503.
SECREST, D., and EASTES, W., 1972, *J. chem. Phys.*, **56**, 2502.
SELWYN, J. E., and STENFELD, J. I., 1969, *Chem. Phys. Lett.*, **4**, 217.
SHARFIN, W., JOHNSON, K. E., WHARTON, L., and LEVY, D. H., 1979, *J. chem. Phys.*, **71**, 1292.
SMALLEY, R. E., LEVY, D. H., and WHARTON, L., 1976, *J. chem. Phys.*, **64**, 3266.
SMALLEY, R. E., WHARTON, L., and LEVY, D. H., 1978, *J. chem. Phys.*, **68**, 671.
STAROVOITOV, E. M., 1990, *Izv. Vyssh. Uchebn. Zaved., Khim. Khim. Tekhnol.*, **33**, 41.
STEINFELD, J. I., 1984, *J. phys. Chem. Ref. Data*, **13**, 445; 1987, *J. phys. Chem. Ref. Data*, **16**, 903.
STEINFELD, J. I., and KLEMPERER, W., 1965, *J. chem. Phys.*, **42**, 3475.
STEVENS MILLER, A. E., CHUANG, C., FU, H. C., HIGGINS, K. F., and KLEMPERER, W., 1999, *J. chem. Phys.*, **111**, 7844.
SULKES, M., TUSA, J., and RICE, S. A., 1980, *J. chem. Phys.*, **72**, 5733.
TAO, F.-M., and KLEMPERER, W., 1992, *J. chem. Phys.*, **97**, 440.
TEICHTEIL, C., and PÉLISSIER, M., 1994, *Chem. Phys.*, **180**, 1.
TELLINGHUISEN, J., 1982, *J. chem. Phys.*, **76**, 4736; 1985, *J. chem. Phys.*, **82**, 4012.
TEULE, R., STOLTE, S., and URBACHS, W., 1999, *Laser Chem.*, **18**, 111.
THAYER, C. A., and YARDLEY, J. T., 1972, *J. chem. Phys.*, **57**, 3992.
THOMMEN, F., EVARD, D. D., and JANDA, K. C., 1985, *J. chem. Phys.*, **74**, 163.
TSCHERBUL, T. V., ZAITSEVSKII, A. V., BUCHACHENKO, A. A., and STEPANOV, N. F., 2003, *Russ. J. phys. Chem.* (in press).
TULLY, J., 1977, in *Semiempirical Methods in Electronic Structure Calculations*, Part A, edited by G. A. Segal (New York: Plenum), p. 199.
URBACHS, W., ABEN, I., MILAN, J. B., SOMSEN, J., STUIVER, A. G., and HOGERVORST, W., 1993, *Chem. Phys.*, **184**, 285.
UZER, T., 1991, *Phys. Rep.*, **199**, 73.
VALENTINI, J. J., and CROSS, J. B., 1982, *J. chem. Phys.*, **77**, 572.
VAN DER BURGT, J. P. N., and HEAVEN, M. C., 1984, *J. chem. Phys.*, **81**, 5514.
VILLARREAL, P., MIRET-ARTÉS, S., RONCERO, O., DELGADO-BARRIO, G., BESWICK, J. A., HALBERSTADT, N., and COALSON, R. D., 1991, *J. chem. Phys.*, **94**, 4230.
WAN, C., GUPTA, M., BASKIN, J. S., KIM, Z. H., and ZEWAIL, A. H., 1997, *J. chem. Phys.*, **106**, 4353.
WILLBERG, D. M., GUTMANN, M., BREEN, J. J., and ZEWAIL, A. H., 1992, *J. chem. Phys.*, **96**, 198.
WILLIAMS, J., ROHRBACHER, A., DJAHANDIDEH, D., JANDA, K. C., JAMKA, A., TAO, F., and HALBERSTADT, N., 1997, *Mol. Phys.*, **91**, 573.
WILLIAMS, J., ROHRBACHER, A., SEONG, J., MARANAYAGAM, N., JANDA, K. C., BURCL, R., SZCZĘŚNIAK, M. M., CHAŁASIŃSKI, G., CYBULSKI, S. M., and HALBERSTADT, N., 1999, *J. chem. Phys.*, **111**, 997.
WOOD, R. W., 1911a, *Philos. Mag.*, Ser. 6, **21**, 309; 1911b, *Philos. Mag.*, Ser. 6, **22**, 469.
XU, Y., JÄGER, W., OZIER, I., and GERRY, M. C. L., 1993, *J. chem. Phys.*, **98**, 3726.
YOURSHAW, I., ZHAO, Y., and NEUMARK, D. M., 1996, *J. chem. Phys.*, **105**, 351.
YOURSHAW, I., LENZER, T., REISER, G., and NEUMARK, D. M., 1998, *J. chem. Phys.*, **109**, 5247.
ZADOYAN, R., LI, Z., ASHJIAN, P., MARTENS, C. C., and APKARIAN, V. A., 1994a, *Chem. Phys. Lett.*, **218**, 504.
ZADOYAN, R., LI, Z., MARTENS, C. C., and APKARIAN, V. A., 1994b, *J. chem. Phys.*, **101**, 6648.
ZADOYAN, R., STERLING, M., and APKARIAN, V. A., 1996, *J. Chem. Soc. Faraday Trans.*, **92**, 1821.
ZADOYAN, R., ALMY, J., and APKARIAN, V. A., 1997, *Faraday Discuss.*, **108**, 255.
ZAMITH, S., MEIER, C., HALBERSTADT, N., and BESWICK, J. A., 1999, *J. chem. Phys.*, **110**, 960.
ŽĎÁNSKÁ, P., ČEK, P. S., and JUNGWIRTH, P., 2000, *J. chem. Phys.*, **112**, 10761.

Zewail, A. H., Dantus, M., Bowman, R. M., and Mokhtari, A., 1992, *J. Photochem. Photobiol.* A, **62**, 301.
Zhao, M., and Rice, S. A., 1992, *J. chem. Phys.*, **96**, 7583.
Zhao, Y., Yourshaw, I., Reiser, G., Arnold, C. C., and Neumark, D. M., 1994, *J. chem. Phys.*, **101**, 6538.